Assessing the health and environmental benefits associated with changes in transportation activities in near-road communities using low-cost sensors

Center for Transportation, Environment, and Community Health
Final Report

By

Mayra C. Chavez, Ph.D.
Evan Williams
Ruey L. Cheu, Ph.D., P.E.
Wen-Whai Li, Ph.D., P.E.

Department of Civil Engineering
The University of Texas at El Paso
El Paso, Texas 79968

May 2022

DISCLAIMER

The contents of this report reflect the views of the authors, who are responsible for the facts and the accuracy of the information presented herein. This document is disseminated in the interest of information exchange. The report is funded, partially or entirely, by a grant from the U.S. Department of Transportation's University Transportation Centers Program. However, the U.S. Government assumes no liability for the contents or use thereof.

TECHNICAL REPORT STANDARD TITLE PAGE

1. Report No.	2.Government Accession No.	3. Recipient's Catalog No.
4. Title and Subtitle Assessing the health and environmental benefits associated with changes in transportation activities in near-road communities using low-cost sensors		5. Report Date June 30, 2022 6. Performing Organization Code
7. Author(s) Mayra C. Chavez(ORCID: 0000-0003-2511-0823) Evan Williams (ORCID: 0000-0002-3384-7836) Kelvin R. Cheu (ORCID: 0000-0002-0791-2972) Wen-Whai Li (ORCID: 0000-0003-1081-1889)		8. Performing Organization Report No.
9. Performing Organization Name and Address Department of Civil Engineering The University of Texas at El Paso 500 W. University Avenue El Paso, Texas 79968		10. Work Unit No. 11. Contract or Grant No. 69A3551747119
12. Sponsoring Agency Name and Address U.S. Department of Transportation 1200 New Jersey Avenue, SE Washington, DC 20590		13. Type of Report and Period Covered Final Report 10/01/2020 - 12/31/2021 14. Sponsoring Agency Code US-DOT
15. Supplementary Notes		

16. Abstract

On-road measurements of four pollutants ($PM_{2.5}$, PM_{10}, NO_2, and O_3) were continuously recorded by three U.S. EPA-certified FEM air pollution monitoring devices installed inside a vehicle traveling repeatedly on the same route in a near-road community. Spatio-temporal on-road air quality data were aggregated and compared to data collected at two fixed stations, one residence located 15 m from the frontage road adjacent to Interstate Highway I-10, and another residential site 300 m from the frontage road. The first objective of this study is to assess the suitability of using the spatio-temporal on-road air monitoring data for representing community exposures to transportation-related air pollutants (TRAPs). While TRAP concentrations observed at a central state-operated site appear to be in good agreement with those observed in the near-road community, concentrations in the community may be better represented by spatio-temporal data generated by an on-road monitor. The second objective of evaluating the feasibility of using on-road air monitors instead of near-road monitors is supported by the facts that pollutants primarily emitted from sources other than traffic, such as PM_{10}, display a different pattern than that of the other three pollutants. On-road monitors successfully detected PM_{10} concentrations near-road as well as in the community that are comparable to the regional background concentrations. $PM_{2.5}$ and O_3 detected by on-road monitors are also comparable to those detected near-road in the community. NO_2 concentrations detected by the on-road monitors varied from the near-road monitors due to the complex interactions with ambient temperature, vehicle emissions, and atmospheric chemical reactions. It seems likely that community exposures to TRAPs can be represented by short-term spatio-temporal measurements using on-road monitors. On-road air pollution measurements provide a rapid assessment of the air quality in a community without installing multiple stationary sites.

17. Key Words	18. Distribution Statement
Traffic Emissions, $PM_{2.5}$, PM_{10} NO_2, O_3, Air Modeling, Air monitoring	Public Access

19. Security Classif (of this report)	20. Security Classif. (of this page)	21. No of Pages	22. Price
Unclassified	Unclassified		

Form DOT F 1700.7 (8-69)

TABLE OF CONTENTS

LIST OF TABLES

LIST OF FIGURES

CHAPTER 1: INTRODUCTION

Urban air pollution is a complex phenomenon in which pollutant concentrations vary spatially and temporally. This may depend on the locations and strengths of emission sources as well as the chemical and photochemical reactions of pollutants in the atmosphere. Micro and macro meteorology of the region and topologic features of the environment also affect air pollution distribution. Regional-scale background concentrations prevailing in the region may also obscure the effects and distribution of urban air pollution. Pollutants emitted from transportation related activities, particularly emissions associated with internal combustion engines, consist of a slew of hazardous air pollutants which pose significant adverse health effects to the population. Exposure to these transportation related air pollutants (TRAPs) could be harmful to human health and the environment. People who engage in outdoor physical activity in a polluted environment are likely to have increased health risks compared to those who have a more sedentary lifestyle, which may be counterproductive to the promotion of physical activity, although the benefits of physical activity outweigh the increased adverse health effects due to airway exposure to the TRAPs [1]–[4]. Different population groups, such as children, elderlies, pregnant women, or people living in near-road communities are especially susceptive to the TRAPs as reported in a number of epidemiological studies [5], [6]. The adverse health effects of TRAPs on human health have been studied in recent years due to public interest and consideration from policy makers, with special interest on school age children. Approximately 3.2 million students attended schools located within 100 m of a major roadway and an additional 3.2 million students attended schools located 100-250 m from major roadways, as reported by Kingsley and his colleagues [7]. Schoolchildren living near busy highways had increased arterial stiffness [8], increased carotid intima-media thickness [9], decreased academic performance [10], increased absenteeism [11], increased clinical asthma symptoms [12], respiratory health [13]–[15], behavioral problems [16], and physical problems [17].

1.1 Background and Motivation

Underserved communities near major roadways may be constantly exposed to these TRAPs and therefore characterization of the spatio-temporal variation of urban air pollution would provide effective pollution control measures to reduce exposure. Air pollutant concentrations are

typically measured with stationary air quality monitors, often few due to high initial and continued maintenance costs. However, the results are never sufficient for conducting an impact assessment in a large study domain. To compensate the shortcoming of insufficient fixed monitoring locations, mobile or on-road monitoring of air quality has been conducted using various instruments and transportation facilities since 2010. Brantley et al [18] provided a good summary of application of on-road air quality monitoring in emission characterization, near-source assessment, and general air quality surveying. On-road monitoring refers to continuous air pollution monitoring using instruments mounting on a moving transportation facility such as pedestrian, bicycle, automobile, utility trucks, train, or any other forms of moving vehicles. Rapid advancements in electronic and communication technologies in recent years have significantly reduced the weight, size, and cost of air quality monitoring instruments while improving the reliability and accuracy of the devices at the same time; it affords the collection and storage of a plethora of special and temporal air pollution data in conjunction with concurrent geospatial locations. This large amount of spatial temporal air quality data could provide better understanding of air quality distribution in the environment and effectiveness of mitigation measures in pollution abatement.

Short-term (1-second or 5-second) on-road data can be used to assess the strength of an emission source if collected closed to the source; averaged to show the spatial trends in a broader area if collected along designated routes, or analyzed together with data collected at fixed stations to evaluate the background air quality trends [18]. Bratley et al [18] illustrated several data processing methods for removing background concentrations from the on-road data and concluded that an average concentration along the route that have low traffic and far from any source could be the best estimate for the urban background concentration. In addition, spatial averaging resulted in smoother concentration gradients and stronger correlations than temporal averaging.

PM concentrations including particle number (PN), black carbon (BC), fine particles $PM_{2.5}$, and particle size were measured using an on-road, bicycle-based monitoring platform during morning and afternoon rush hours to explore patterns of exposure while cycling [19]. The study concluded that instantaneous traffic volumes quantify the increase in particle concentrations associated with each passing vehicle. Acute, high concentration exposure events could take place by a moving truck which could cause an increase of 31,000 particles/cm^3 in PN, 1.0 μg/m^3 in $PM_{2.5}$, and 1.6 μg/m^3 in BC. It was also observed that PM concentrations were correlated with street functional class and declined within distances from a major road. While the fine PM

surrogates (PN and BC) decreased by approximately 20% one block away from major roads to adjacent local roads, $PM_{2.5}$ mass concentration showed small decrease by <10% from the major road to a distance 400 m away from the road, based on the difference observed in the central concentration tendencies (as represented by the mean concentrations). The significant difference in the concentration decreases (~20% in one city block v.s. ~10% in 400 m) for PM surrogate (PN and BC) and $PM_{2.5}$ is attributed to the high traffic on the arterial roads, where the emissions are primarily composed of UFP that is characterized by high PN and BC. However, the more regional nature of $PM_{2.5}$ pollution is characterized by the urban background $PM_{2.5}$ concentrations.

Yu et al characterized the spatial and temporal variation of four TRAPs (BC, $PM_{2.5}$, PN, and CO) in an urban community by taking 5-minute averages of pollutant concentrations collected by pedestrian walking on designated routes [20]. Each reported concentration in this study represents approximately a spatial average of 520 m, based on an average adult walking speed of 6.4 km per hour. Yu et al concluded that the spatio-temporal characteristics of the collected TRAP concentrations were consistent with findings in previously reported studies. Another on-road monitoring campaign was conducted in Montreal, Canada to evaluate the health effects of transportation emissions [21]. On-road measurements of O_3 and NO_2 in this study were carried out by walking and bicycling. The authors discovered that O_3 and NO_2 concentrations measured by the on-road sensors were consistent with the data reported by the city using refined, regulatory compliant instruments and that the diurnal variations of the two pollutants were consistent with the expected diurnal patterns in the city. Similar techniques were applied by strapping low-cost sensors on the wrist of an operator for on-road CO and NO_2 measurements in a near road air pollution study by McKercher and Vanos [22]. However, they reported low confidence in low-cost sensors and advocated developing data processing firmware for citizen science low-cost air monitoring. Wei et al deployed on-road sensors onto buses to monitor NO, NO_2, CO, and $PM_{2.5}$ concentrations along 10 major routes in Hong Kong [23]. Baseline extraction methods were used to separate background and local concentrations, and by these methods it was shown NO and NO_2 are dominated by local emissions. This conclusion would indicate that NO_2 concentrations are likely to be higher along the frontage road where one would expect higher local emissions.

In another study, taxis were used as the vehicle for on-road monitoring by installing laser PM sensors on fifty taxis to map PM pollution in a city [24]. The study concluded that the on-road measurements provide comparable data to that reported from fixed monitoring stations and suggested the use of on-road monitoring system for providing exposure concentrations in assessing public health risks and developing air pollution control policies. A similar study conducted in Taipei, Taiwan collected traffic-related air pollutants on an on-road platform, specifically BC, ultrafine particles (UFP), $PM_{2.5}$, and CO [25]. Lung deposition surface area (LDSA) was also used to represent the surface area of particles that deposit in the alveolar region and assess the negative health impact it would have on humans. It was found UFP concentrations and LDSA were up to two times higher on high-traffic routes than low-traffic routes, constituting a significant impact on human health commuting on the high-traffic routes daily.

TRAP concentrations were also measured on an urban road with medium traffic volume of ~400-800 vehicles/hour and an average speed of 40 km/hr in Australia [26]. On-road air samples were collected immediately adjacent to the road (i.e., within 1 m from road markings and the curb). On-road $PM_{2.5}$, PM_{10}, and O_3 concentrations observed during this short-term study (9 hours during the day for 2 days) were low and well below the WHO guideline concentrations and the NAAQS of U.S. The relatively small increases in on-road $PM_{2.5}$, PM_{10}, and O_3 concentrations from their respective urban backgrounds imply the prevalence of urban background PM and O_3 concentrations and that on-road TRAP concentrations are less affected by the variability in local vehicle emissions, traffic, and meteorological conditions. Furthermore, statistical analyses employed in the study also suggest that on-road NO_2 and O_3 concentrations were largely driven by atmospheric photochemistry processes at vehicle exhausts.

Another study collecting BC, UFP, and $PM_{2.5}$ attributed differences in the concentrations between background and local emissions to the traffic and concluded that traffic was actually the dominant source of air pollution [27]. It also found that with enough passes it can create a projection of the air pollution patterns within the community, as well as identify high pollution zones that should be followed-up with increased monitoring or actions taken to reduce pollution.

Zhao et al used 260 vehicles equipped with on-road monitoring to collect real-time, spatially resolved $PM_{2.5}$ concentrations in Beijing, China [28]. Machine learning was used to create a map of air pollution over the city and identify hotspots. On-road data were also compared with data recorded at stationary monitoring sites and on-road and near-road data were found to be well

correlated, with the coefficient of determination between on-road and near-road data ranging from 0.56 to 0.80.

TRAP concentrations were also measured on freeway as well as on the access (or frontage) roads. Baldauf et al [29] conducted a study to determine the influence of noise barriers on both on-road and near-road community in Phoenix, Arizona. TRAP concentrations were measured in the study using on-road and fixed-site monitors along two interstate freeway segments (AADT of ~ 120,000-140,000 for weekday, and ~100,000 for weekend). Each segment contains one road section with noise barrier and another section without noise barrier. While the study showed that pollutant concentrations behind the roadside barriers were significantly lower than those measured in the absence of barriers, the reported on-road and near-road TRAP concentrations without noise barrier (Figure 3 of Baldauf et al [29]) display a comparison of TRAP concentrations on the highway to those measured on the access (or frontage) road that is parallel to the highway without a noise barrier. Although $PM_{2.5}$ was not measured, $PM_{2.5}$ surrogates (BC and UFP) were measured in the study. While meteorological and traffic conditions could influence the distribution of pollutant concentrations from the highway, a decrease trend was observed with or without a noise barrier. The PM surrogate concentrations were found to be reduced by ~50% within 50 m from the freeway under all wind directions. Changes in wind direction and local traffic conditions on both the freeway and access roads contributed to high variability in individual measurements on the access roads, however, BC and UFP concentrations observed on the access roads were relatively steady and indistinguishable from those observed immediately behind the noise barrier.

The rapidly evolving on-road air monitoring technique has gained a strong foothold in air quality monitoring due to its unique nature of providing instantaneous temporal and spatial measurements. Nevertheless, some inherited challenges remain to be resolved, primarily in the relationship between its measurements and the conventional time-averaged air quality data typically collected at fixed stations. First, spatial resolution associated with on-road measurement is a major concern in on-road sampling. The distance between two sampling points (spatial resolution) depends strongly on the vehicle speed and idle time. For instance, Shi et al suggested an optimal spatial aggregation of 300 m based on their study in Hong Kong [30]. Second, the representativeness of a point measurement in space and time remains undefined. A point

measurement collected along a long segment of a roadway could only represent an instantaneous observation of a three-dimensional concentration dataset that varies in space (1st and 2nd dimension) and time (3rd dimension). Third, TRAPs decrease rapidly from highway to near-road locations. Karner et al analyzed 41 roadside monitoring studies between 1978 and 2008 and concluded that almost all pollutants decay to background levels at a distance 115 m to 570 m from the edge of the road and the decay rate varies from one pollutant to another [31]. Venkatram et al showed that the concentration of an inert pollutant decays rapidly to less than 1/5 of its initial strength in 100 m in the direction normal to the roadway [32]. Recently, Cahill et al showed the downwind PM could be essentially undiluted at distances well beyond 200 m due to many uncontrollable factors, such as the existence of sound walls for at-grade freeways, elevated or filled section of a freeway, canopy vegetation, and classification of atmospheric stability condition [33]. Thus, it is of paramount importance to understand the relationship between the data collected using the on-road technique and that reported from a nearby fixed station. [34].

1.2 Research Objectives

This project provides support for estimating near-road concentrations using on-road monitoring traveling on fixed paths. The study tests two hypotheses: 1) Community exposures to transportation pollutants can be represented by short-term spatio-temporal measurements using on-road air monitors; and 2) near-road receptors can be represented by on-road air monitors. The objectives of this study are to 1) provide concentration estimates for a community using on-road air pollutant monitoring, and 2) evaluate associations of short-term TRAP concentrations between near-road and on-road receptors. The results will be used to develop community exposure maps for the study area.

CHAPTER 2: METHODOLOGY AND STUDY DESIGN

This study was designed and conducted to test the hypotheses in a well-controlled residential community located near a busy interstate highway. The implementation of this project provides a cost and time effective method for estimating the burden of traffic pollution on a near-road community's health. Three tasks were implemented in this study including:

Task 1: Instrumentation Setup and Route Selection

A route was selected to cover the community as well as the near-highway environment in the selected community. A transit vehicle was equipped with three types of air monitors for $PM_{2.5}$, PM_{10}, NO_2, and O_3 monitoring. All instruments were calibrated before the study against the data recorded at a state-operated air monitoring station using federally referenced method (FRM) to ensure consistency in data quality between the data collected in this study and those collected with FRM instruments.

Task 2: Air Pollution Measurements

TRAP measurements were conducted on-road and at two fixed locations along the route. Identical instruments were used at two fixed sites as well as inside the transit vehicle. A residence located approximately 15 m from the frontage road adjacent to the westbound Interstate Highway I-10 (hereinafter the Frontage Site) was selected for comparison of on-road and near-road TRAP concentrations. A second residence in the same community, approximately 300 m from the Frontage Site and the highway, was selected for evaluation of TRAP concentrations in the residential community (hereinafter the Residential Site). TRAP concentration measurements at the two selected locations continued throughout the study period.

Task 3: Data processing and Report preparation

The on-road data were processed along with the GPS data for generating concentration surfaces. The on-road data were compared to data collected at the near-road sites. Statistical analyses were conducted to examine the associations between the on-road and near-road TRAP data.

2.1 Study Design and Route Selection for On-road Air Monitoring

This study was conducted in El Paso, Texas near the main campus of the University of Texas at El Paso (UTEP). Prior to the monitoring campaign all air quality instruments were calibrated against data concurrently collected by TCEQ using the U.S. EPA FRM-designated

instruments at a state-operated air monitoring site, the CAMS 12 site. All instruments were located within 3 m from the FRM instruments. They were positioned inside the fenced area and outside the UTEP field air monitoring laboratory, which shares a common chain fence with CAMS 12. One set of the calibrated air monitoring instruments were relocated inside the UTEP air quality on-road station. The UTEP air quality on-road station (housed inside a Chrysler cargo van) was modified to house the instruments with an external air inlet on top of the roof (Figure 1). The inlet was positioned approximately 0.6 m above the top of the van to avoid the upwind turbulent cavity zone formed on the roof while vehicle is moving and to minimize possible cross contamination of tailpipe emissions while vehicle comes to a halt. The route for on-road air monitoring is shown in Figure 2. The route was designed to be a route of approximately 16 km to include segments of frontage road of I-10, business districts, and near-road residential neighborhoods.

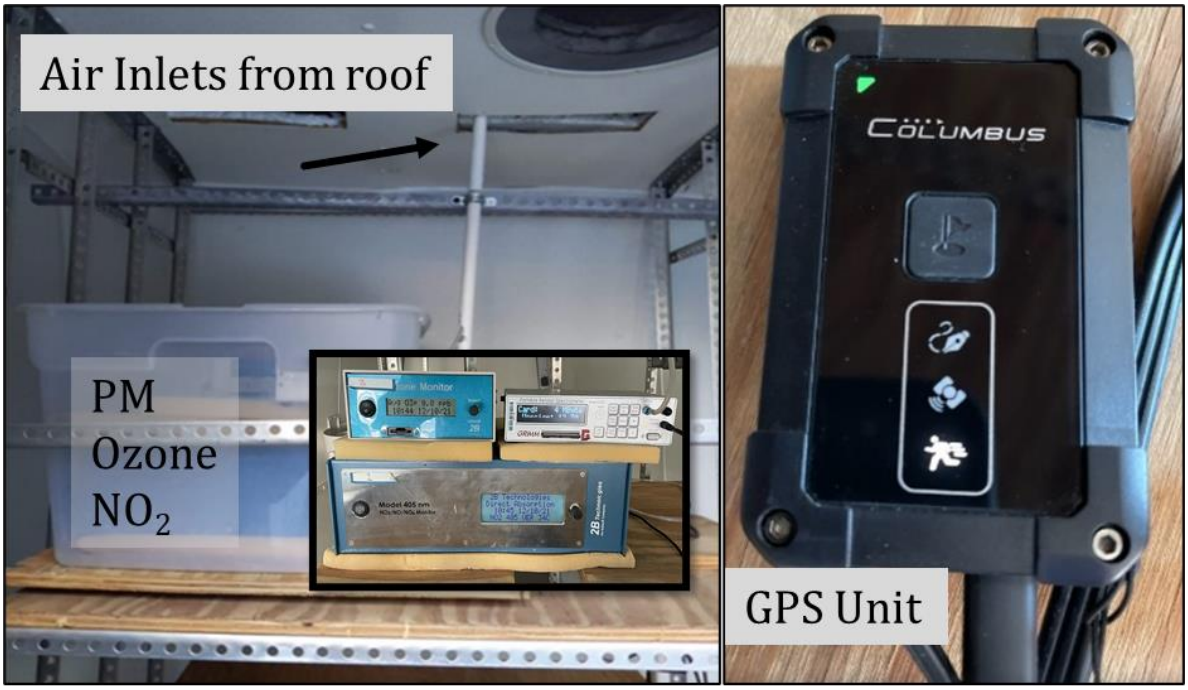

a) Instruments inside mobile monitoring unit

b) Outside view of mobile monitoring unit

Figure 1 Air Quality On-road Station

On-road monitoring was conducted along a designated route in a community adjacent to Interstate 10 (I-10) shown in Figure 2. The route was directed through the community and passed alongside the Residential Site which is 350 m away from I-10, as well as the Frontage Site. Both locations are shown in Figure 2. The vehicle travelled along an arterial road (Mesa Street) with

multiple traffic lights, a moderate traffic surface street (Montana Ave), streets of different traffic intensity, and the frontage road of I-10. The total length of the loop is approximately 10 km.

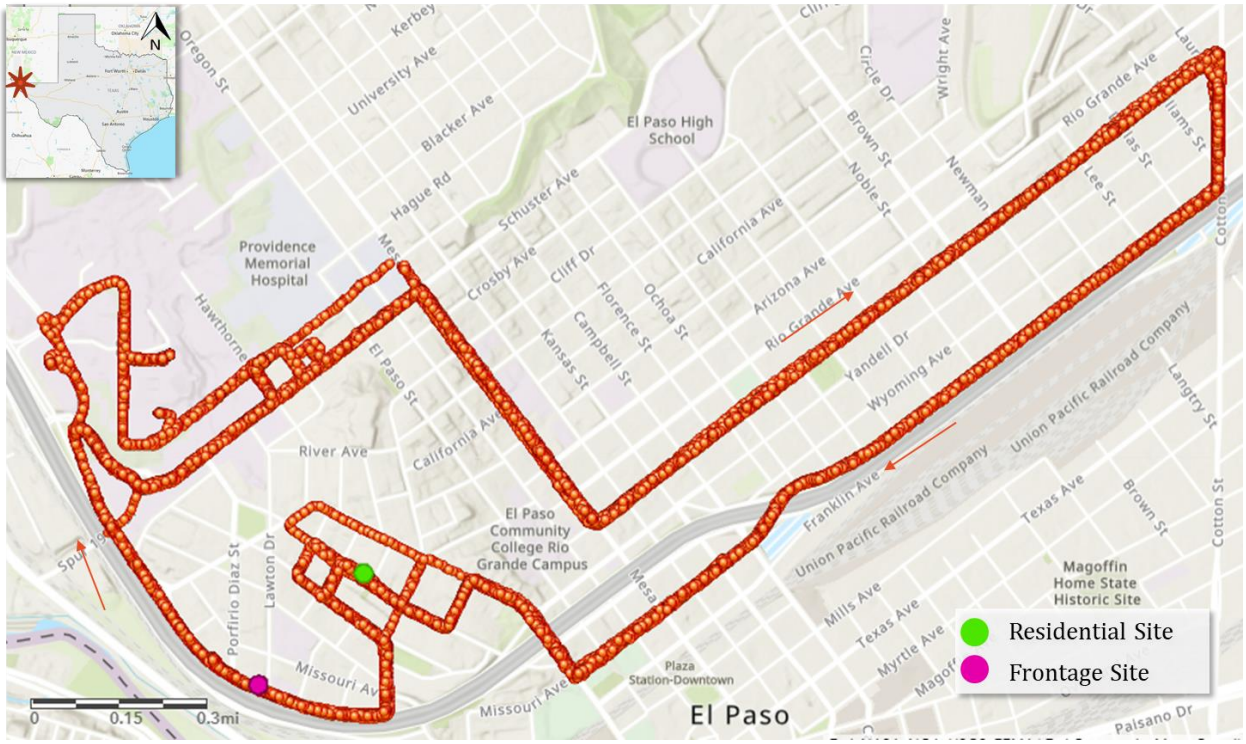

Figure 2 Study area and On-road Monitoring route

Each trip lasted about 20 minutes including stop-and-go at all traffic intersections. The air monitoring campaign began on November 18 and ended on December 4, 2021, for a period of 13 days; this excludes any holidays. A total of 330 trips were conducted during this field study period resulting in around 110 hours of simultaneous collected, validated data of $PM_{2.5}$, PM_{10}, O_3, NO_2, time, and GPS information. Table 1 summarizes the number of loops driven during the on-road monitoring as well as the total number of hours of pollutant data collected.

Table 1 Number of Loops and Hours Driven

	19-Nov	20-Nov	22-Nov	23-Nov	24-Nov	29-Nov	30-Nov	1-Dec	2-Dec	3-Dec	4-Dec	Total
Loops	30	30	30	30	30	30	30	30	30	30	30	**330**
Hours Driven	12	12	12	12	12	12	12	12	12	12	12	**132**

Historical traffic data for 2017, as reported by TxDOT, is summarized in Figure 3. The annual average daily traffic (AADT) at a location is represented with dots on the map. AADT along the section of I-10 from Cotton Street to where the Frontage Site is located varies from 130,000 to 170,000. Traffic in downtown El Paso was around 25,000 AADT on the major thoroughfares, and from 3,000 to 10,000 AADT on the surrounding collector streets. As expected, traffic is much less in the Sunset Heights Residential Community, around 2,000 – 4,000 AADT. The Sunset Heights Residential Community is defined as the area within the green shape.

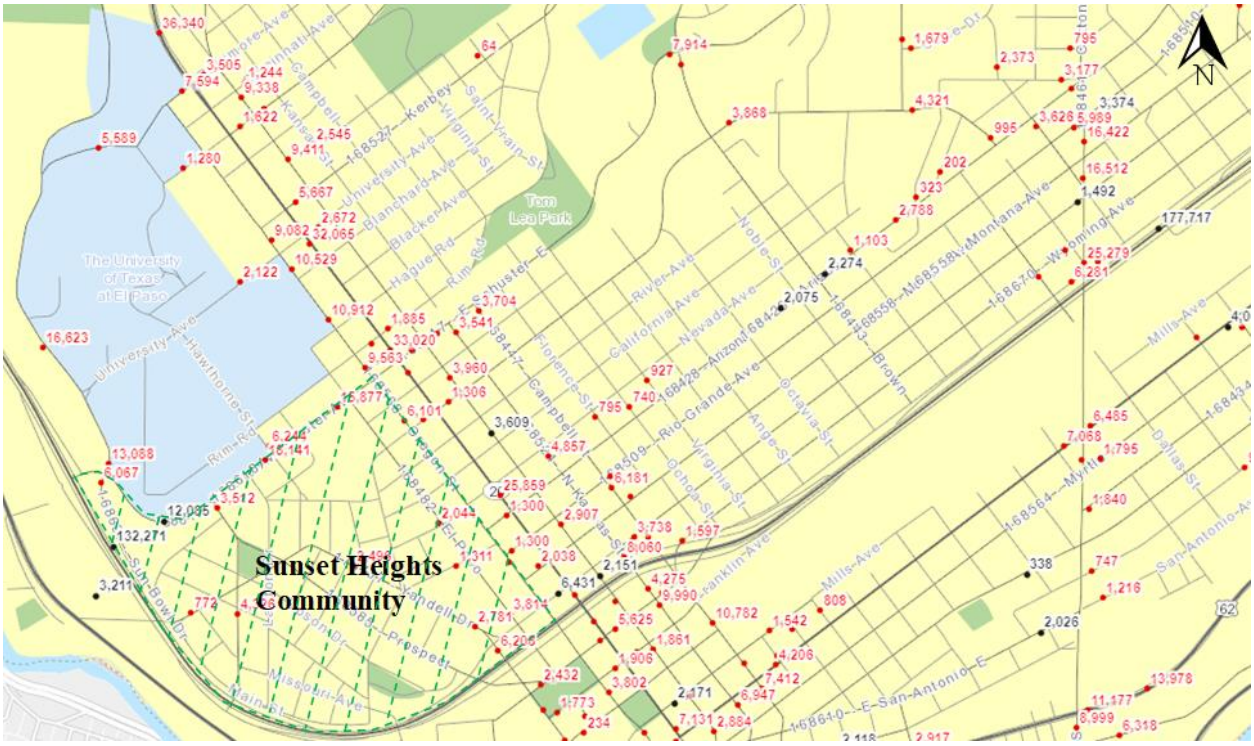

Figure 3 2017 Annual Average Daily Traffic (AADT)

2.2 Air Quality Data Collection

2.2.1 Instrumentation and Setup

Air quality data were collected by three different monitoring instruments. NO_2 was measured using 2B Technologies NO_2/NO/NOx Monitor [35]. O_3 was measured using 2B Technologies Model 202 O_3 Monitor [36]. Particulate matter was measured using GRIMM

Portable Laser Aerosol Spectrometer and Dust Monitor [37]. All three instruments are U.S. EPA FEM-designated air monitors.

2.2.2 Instrumentation Data Correction

Prior to any field measurement, instruments were calibrated against pollutant data collected at the TCEQ-operated CAMS 12 site using FRM designated instruments. The monitors were placed in the UTEP field laboratory, a fenced area with a trailer equipped with electricity and is immediately adjacent to CAMS 12. All instruments were placed within 6 m from their respective FRM devices for a side-by-side comparison, as shown in Figure 4. Collocated data were collected continuously at this site for all instruments for a period of 7 days for developing a correlation relationship between each FEM instrument and its respective FRM instrument.

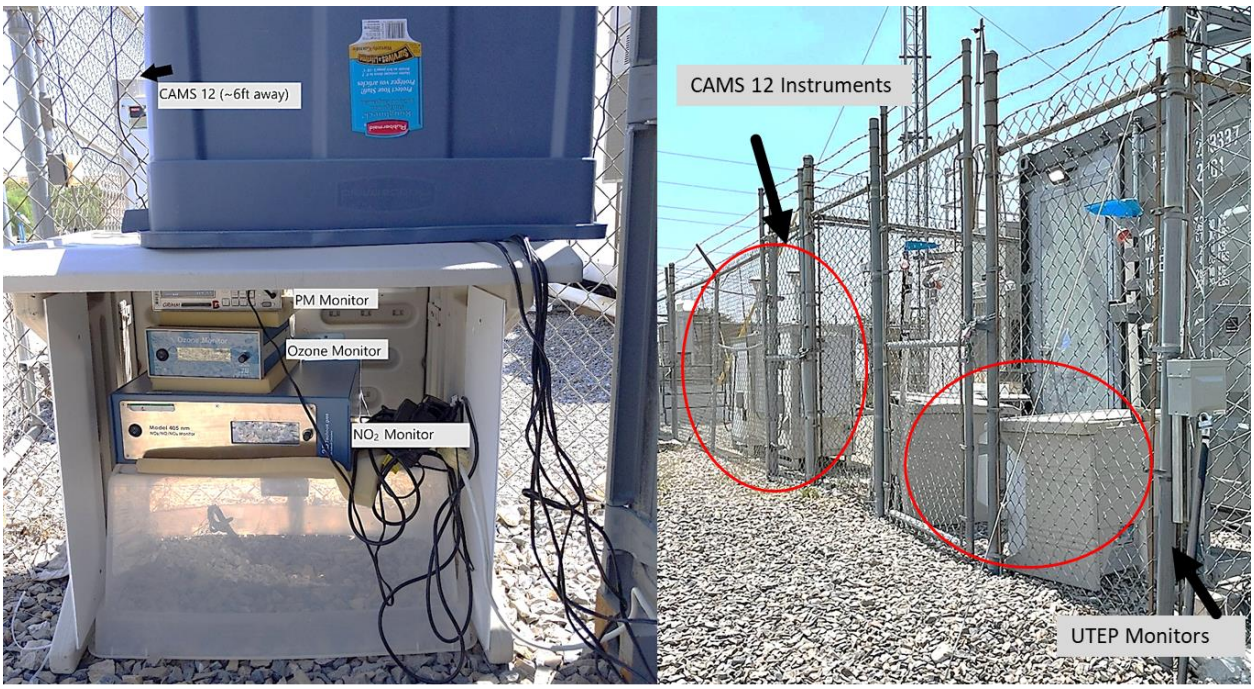

a) Monitors used in UTEP study b) zoomed-out view showing CAMS 12 instruments 6 ft away

Figure 4 Data Correction set-up of monitoring instruments a) Monitors used in UTEP study b) zoomed-out view showing CAMS 12 instruments 1.8 m away

Summarized in Table 2 are the correction data displaying consistent performance of the instrument with negligible electronic drift. The final correction equation for each monitor was developed using the whole set of correction data. Table 2 also displays the final correction equation

and associated R^2-value used for data processing. Figure 5 shows the Pearson scatter plots for the correction period and how the correction statistics were developed.

Table 2 Correlation and Regressions Analysis with CAMS 12 Data

	On-road			**Residential**			**Frontage**		
	R^2	Slope	Intercept	R^2	Slope	Intercept	R^2	Slope	Intercept
PM_{10}	0.83	1.41	7.56	0.79	4.46	6.34	0.96	0.42	9.31
$PM_{2.5}$	0.82	0.75	3.65	0.80	1.57	3.89	0.90	0.63	1.28
O_3	0.99	1.05	-1.15	0.98	0.92	4.78	0.99	1.10	-2.29
NO_2	0.83	0.95	3.18	0.57	0.69	2.59	0.60	0.61	3.27

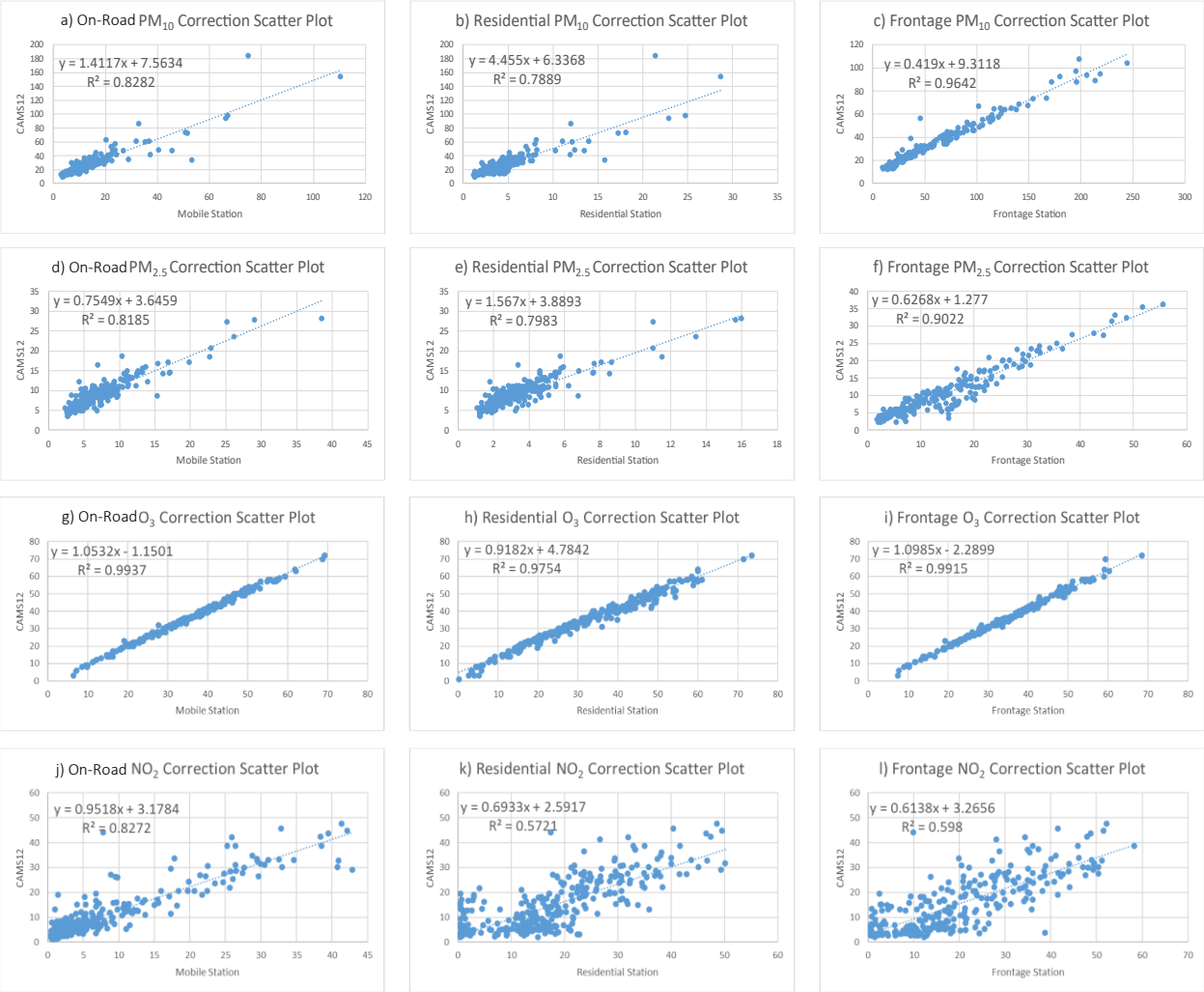

Figure 5 Pearson Correction Scatter Plots

2.2.3 Field Study

One set of instruments was installed inside the on-road station driven on the route. Monitors were placed on a shelving unit with soft pads that helped attenuate vibration of the instruments during on-road monitoring. This shelving unit also raised the height of the instruments, which allowed the inlet tubes of the monitors to reach outside via a pipe that went through the roof and reduced the length of the tube to avoid unnecessary PM mass loss. Inlet tubes were also shielded from rainwater. NO_2 readings were collected every 10 seconds, O_3 every 5 seconds, and $PM_{2.5}$ and PM_{10} every 6 seconds. These intervals are the lowest allowed by each monitor. A Columbus P-1 Professional GPS Data Logger was also placed with the monitors, which collected longitude, latitude, and speed every second. At the start of every day, the monitors were turned on and allowed

to run for 30 minutes before beginning the on-road monitoring route. This 30-minute wait period allowed the monitors internal temperatures to stabilize so that possible electronic interference by temperature fluctuation could be minimized.

Another set of the air monitoring instruments was placed at a residence within the community that was approximately 300 m away from the interstate. This site labeled “Residential Site” is shown in Figure 6. Also shown in Figure 6 is the overview of the site in relation to the street. As is noted, the actual residence is around 5 m above the street level. The set of instruments at this site collected $PM_{2.5}$, PM_{10} O_3, and NO_2 data every 5 minutes and ran for the entire collection period, day and night. The instruments were protected from rain and wind by a housing unit, which also provide shade for the instruments to maintain an adequate range of operating temperature.

a) Residential site monitoring station b) View of Residential site on-road

Figure 6 Instruments at Residential Site and view from the road

A third set of instruments was placed at a residence immediately adjacent to the interstate I-10. This site labeled “Frontage Site” was approximately 13 m from the road segment which is the frontage road of I-10. This section of the neighborhood is also around 15 m higher than the interstate. This site and view from the road are shown in Figure 7.

a) Frontage site monitoring station b) View of frontage site on-road

Figure 7 Instruments at Frontage Site and View from the road

2.3.4 Data processing

As stated previously, each of the three monitors had a different lowest resolution for recording data points. In order to obtain synchronized data among the monitors and the GPS unit, the pollutant data were interpolated between two consecutive readings by assigning the ending reading to all 1-second data in the interval between the two readings. For example, the last data point recorded for $PM_{2.5}$ was used to represent each of the previous 6 seconds. This 1-second data were used to spatially plot pollutant concentrations and create averages in 25-m hexagonal bins. An example of the hexagonal bins is shown in Figure 8 for the 1-second NO_2 data points collected at a segment of the streets along the route during the whole study period. It can be seen in Figure 8 that a few data points are dispersed off the main route. This is attributed to occasional route changes due to some unexpected construction and/or incidents which forced the vehicle operator to slightly alter the route.

ArcGIS averages all data points within 25 m into hexagonal bins which were chosen to create a more even coverage of point aggregation compared to square areas. Data points provided by the GPS were slightly off from the base layer map due to the projection of the map in the ArcGIS software. The high number of 1-second data points over a daily period made visual analysis difficult and the hexagonal bins provide a more general view of the pollutant

concentrations along the route. The 1-second data points had slight spatial variations due to projections onto the mapping software and GPS unit's resolution level. Hexagonal bins allowed for an even distribution of points to represent the road segments.

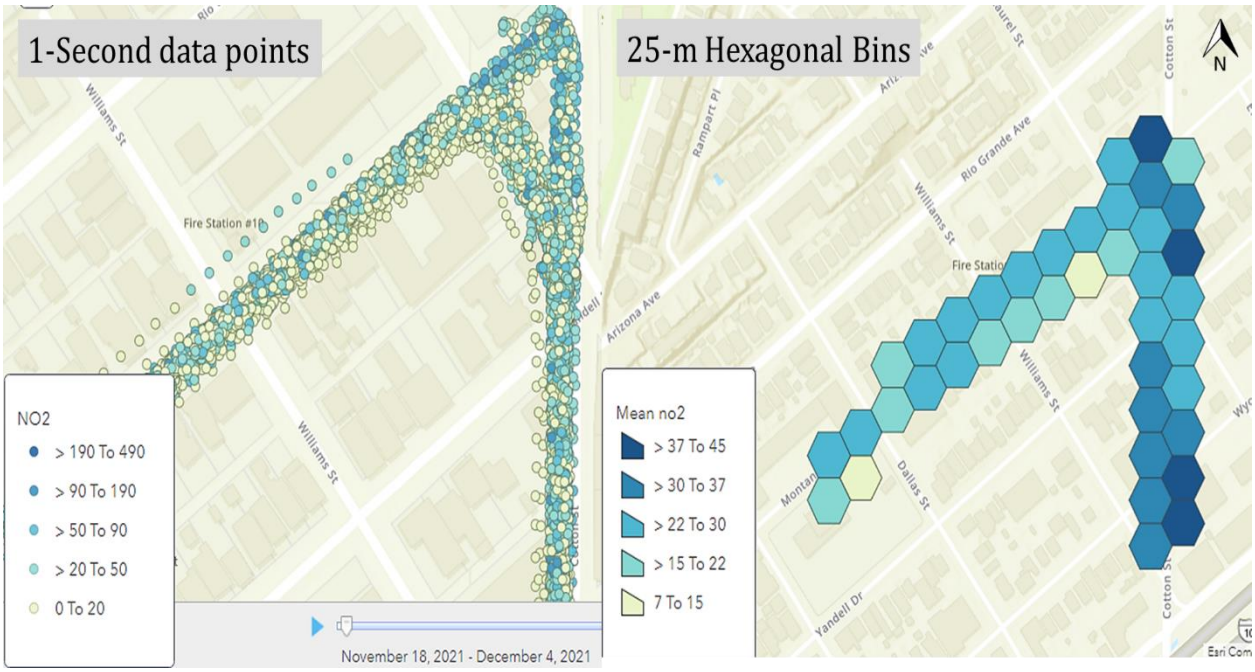

Figure 8 One-second data points to Hexagonal bins for averaging

CHAPTER 3: DATA PROCESSING AND RESULTS

3.1 Air Quality Data Visualization and Database Structure

Figure 9 provides an illustration of the locations of NO_2 data collected from all runs in a typical road segment. Each dot in Figure 9 represents the location and magnitude of a NO_2 data point, recorded along with the GPS location and time of the day. The density of the data point in a road segment varies depending on the frequency of trip, traffic condition, and the speed of the vehicle.

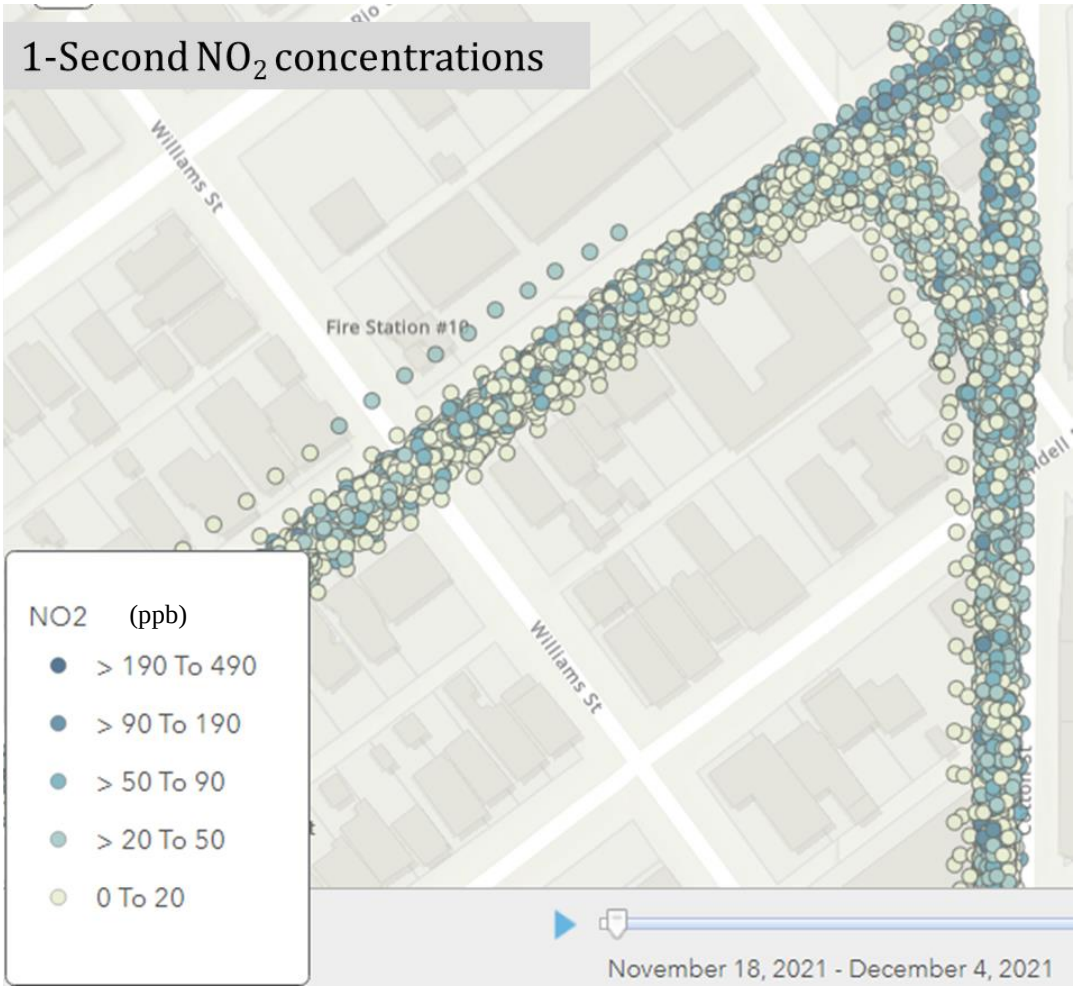

Figure 9 Road segment showing 1-second $PM_{2.5}$

Once each recorded pollutant concentration was extrapolated to a 1-second resolution, a database was created for each day of the on-road monitoring campaign along with the longitude

and latitude of each data point. This database was used in the spatial analysis done using ArcGIS as well as any statistical and data analysis using Jupyter Notebook (Python), R Studio, and Excel. The air pollution data collected during this study was processed for accuracy and completeness. Values reported by the monitors as negative, due to being below the monitors' method detection limits, were corrected. The reported concentrations can be negative due to zero drift in the electronic instrument output, data logger channel, or correction adjustments to the data. Slightly negative values were automatically set to 0.5 (i.e., 1/2 of the detection limit), unless the negative values were more than three consecutive values; these were considered missing data. The finalized air pollution data were also adjusted using the correction equation for each instrument found from the correction data.

3.2 Air Quality Data Results

3.2.1. Overview of On-road Data

Summary of the hourly pollutant concentration along all routes during the study period is presented in box plots in Figure 10 where the distribution of data for the hour are marked in terms minimum (Q1-1.5•IQR), first quartile (Q1), median, third quartile (Q3), and maximum (Q3+1.5•IQR). Figure 10 shows the temporal averages of the pollutant concentrations for the hour along the route covered by the vehicle. Each data point represents the average of the time-varying pollutant concentrations along the route in an hour. The white circle represents the mean value for hourly pollutant during that hour. Blue dots represent minimum and maximum values, while the end of the whisker plot represents the quartile value. As expected, the diurnal variation of $PM_{2.5}$ concentration resembles closely to that of PM_{10} and the overall average of $PM_{2.5}$ concentration is approximately 30% of PM_{10}. In El Paso, PM, in general, peaks in the early morning hours around 6 am and again in the early evening hours around 6 pm due to the traffic intensity [38]. The ratio for $PM_{2.5}$ to PM_{10} is around 0.25 [38], [39] due to the high fugitive emissions from geologic sources (surrounding desert) and traffic-enhanced emissions of road dust. On-road $PM_{2.5}$ concentrations are expected to be closely associated with traffic. In El Paso, as well as in many major cities, traffic intensifies in the early morning and late afternoon which coincides with the diurnal occurrences of $PM_{2.5}$ peaks.

NO_2 data in general show a steady increase and peaks in the evening. NO_2 is a product of combustion and an EPA criteria pollutant primarily emitted from vehicle exhausts. It is a precursor in the O_3-NO_2 photolysis. NO_2 is rapidly depleted in the atmosphere during the day especially under strong solar radiation to form O_3. NO_2 begins to accumulate after sunset when the O_3-NO_2 photolysis ceases to function. In the meantime, O_3 begins to increase in the morning when the sun rises, peaks in the early afternoon when the solar radiation peaks and decreases to the minimum after the sunset. Figure 10c and Figure 10d illustrate the O_3-NO_2 cycle for the Paso del Norte region. It also shows that NO_2 steadily increases from the morning, maintains at an equilibrium level throughout the day, and begins to peak in the late afternoon. The variation shows the balance between the recurring traffic emissions and NO_2 photolysis during the day. As is observed in later sections, O_3 measured by on-road monitoring is highly correlated with O_3 measured at any near-road site in the study area. This further exemplifies the homogenous distribution of O_3 in the region, as compared to the concurrent TCEQ O_3 data.

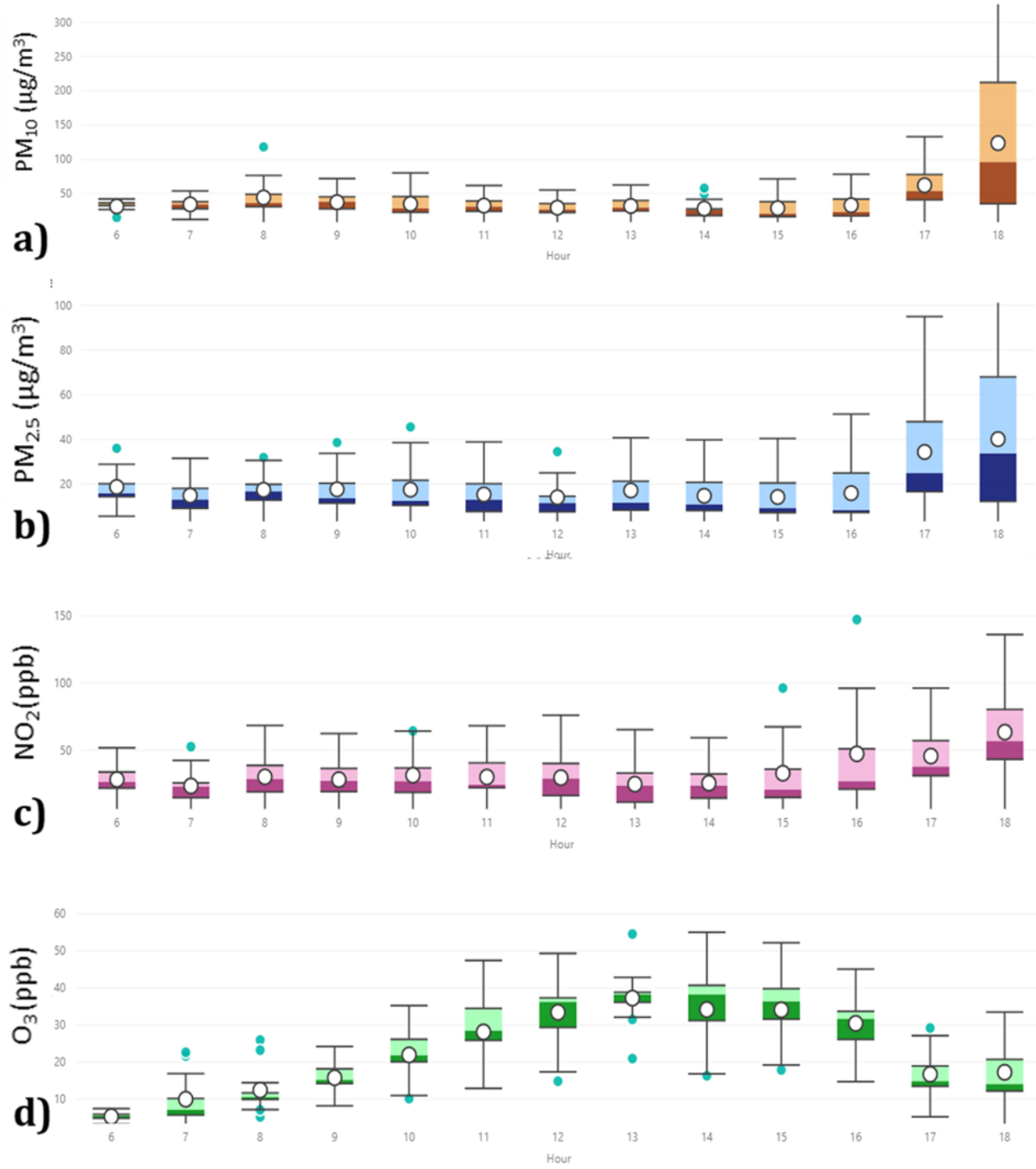

Figure 10 Hourly Boxplot: Pollutant data for all study period: minimum (Q1-1.5•IQR), first quartile (Q1), median, third quartile (Q3), and maximum (Q3+1.5•IQR)

3.2.2. Spatio-temporal averages of on-road concentrations

Figure 11 shows the time-averaged spatial distribution of all four pollutant concentrations, as measured along the on-road monitoring route. Each of the four panels in the figure represents the average of all points for a specific pollutant collected during different times within the 25-m hexagons discussed previously. The air monitoring campaign started on November 18th and ended on December 4th, 2021. It can be seen that PM values (both $PM_{2.5}$ and PM_{10}) appear at high concentrations at the same locations on the route. These locations can be identified as traffic intersections in major business districts and downtown El Paso, frontage roads along the I-10, and UTEP parking lot. PM is seen with higher values along parts of the route with more intersections in the figure, whether free-flowing or stop-and-go. NO_2 values seem to peak at intersections and stops on the on-road monitoring route, at Kansas Street intersections with Montana or in downtown as well as in the section of Cotton Street and I-10. O_3 concentrations, in general, are the most ubiquitous on the on-road monitoring route.

This visualization helps show hotspots at different locations in the study in a more generalized term over the study period. In the study period PM_{10} appears highest at the most congested arterial, Mesa Street, and at various intersections. $PM_{2.5}$ peaks at these locations as well. NO_2 peak values for the period are clustered and evident especially at intersections, near the highway, and a roundabout location on the on-road monitoring route. This increase in NO_2 may be attributed to the stop and acceleration of vehicles as they drive through the roundabout. O_3 had a more uniform distribution on the on-road monitoring route, showing slightly higher values where the vehicle was operating at higher speeds, and especially in the Northwest section near the Interstate. It is also of note that NO_2 and O_3 appeared to peak at opposite levels. Areas along the on-road monitoring route that have higher levels of NO_2, coincide with areas where O_3 is slightly lowest.

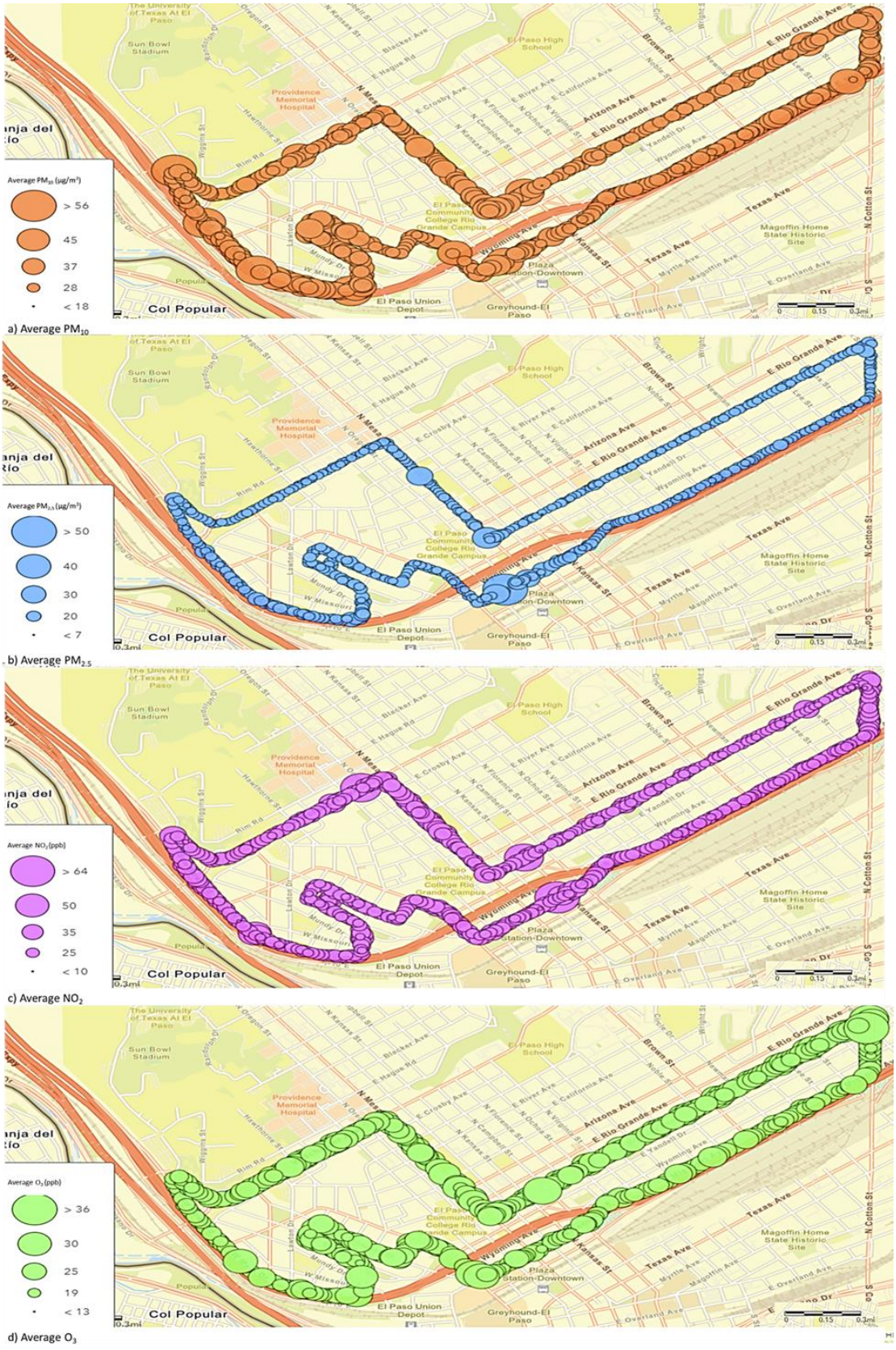

Figure 11 All-Period average of on-road concentrations, a) PM_{10}, b) $PM_{2.5}$, c) NO_2, d) O_3

3.2.3 Comparison of Stationary Site Measurements: Meteorological Parameters and Pollutant Concentrations

Hourly pollutant data at the Frontage and Residential Sites were analyzed comparing the influence of two meteorological parameters, wind speed and wind direction. These parameters were obtained from the TCEQ reference station CAMS 41 located around 4.5 km away. The concentration rose plots are used to visualize this relationship for PM_{10}, $PM_{2.5}$, NO_2 and O_3, as shown in Figure 12. PM_{10} and $PM_{2.5}$ concentrations were high during low wind speed hours when stagnation and temperature inversion were likely to occur. It can be seen in the plots that northeasterly winds prevailed during the study period and high concentrations for all four pollutants occurred either at low-to-calm conditions or under northeasterly winds while both Frontage and Residential Sites are upwind of I-10. This implies that vehicle emissions from I-10 does not necessarily contribute the high pollution concentrations at these two locations or in this near-road community. It is interesting to observe in Figure 12d that high O_3 concentrations occur during strong westerly and northeasterly winds indicating that high O_3 occurred ubiquitously regardless the relative position of the site with respect to the highway.

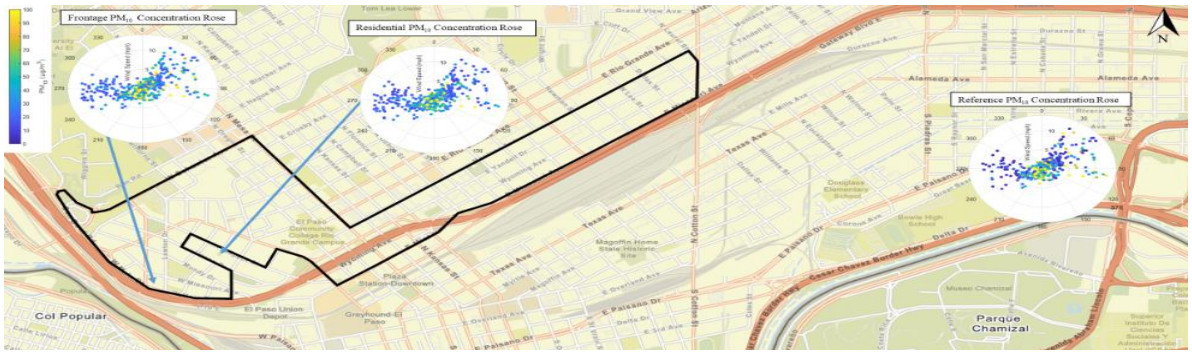

a) Hourly Average PM_{10}

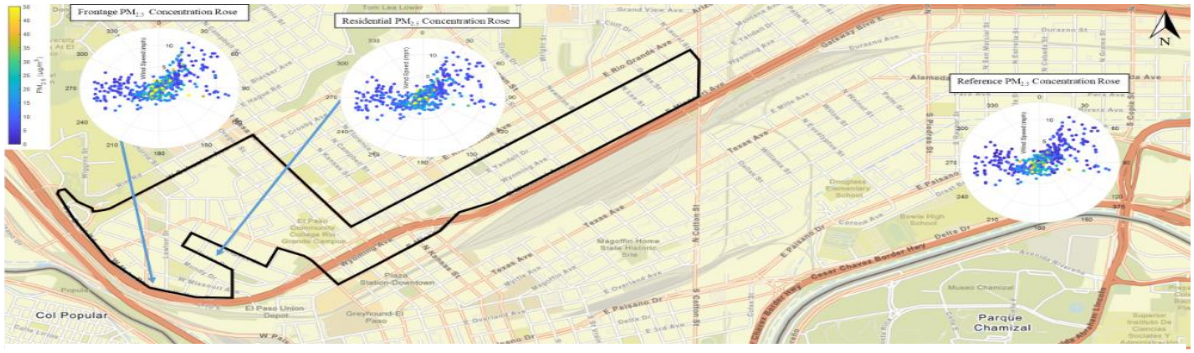

b) Hourly Average $PM_{2.5}$

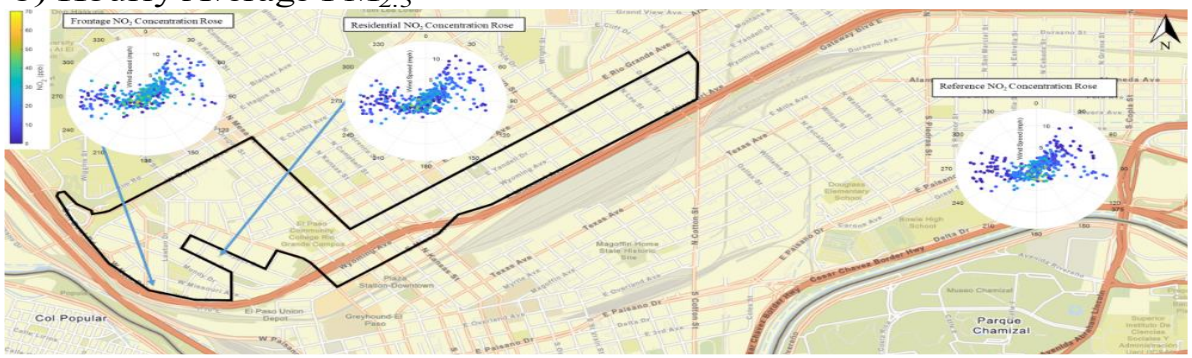

c) Hourly Average NO_2

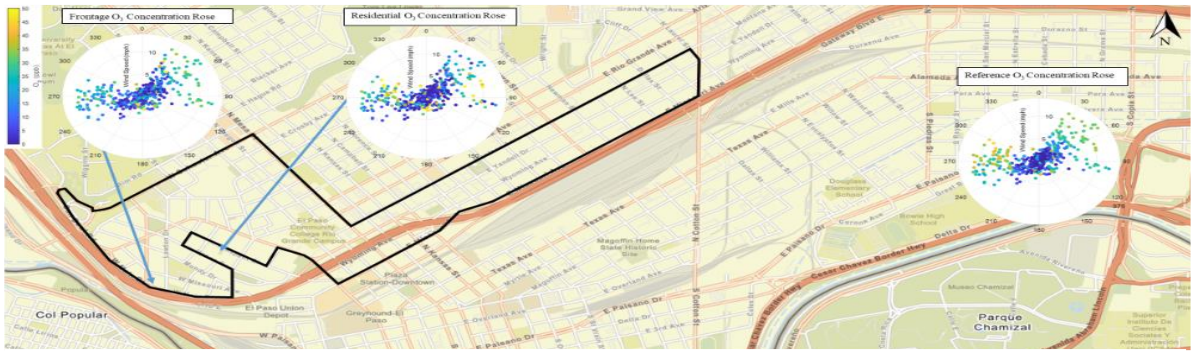

d) Hourly Average O_3

Figure 12 Concentration Polar Plots of Hourly PM_{10} and $PM_{2.5}$ and Wind Data

Figure 13 through 15 show the concentration plots with respect to wind direction and time of the day at the Frontage, Residential, and Reference Site (CAMS 41), respectively. The diurnal variation of the pollutant concentrations is shown in these polar plots where the radial direction indicates the time of the day (Hour 0:00 to 23:00) and the angular direction represents the wind direction. The magnitude of the concentration is marked in accordance with the color code provided in the figures. Figure 13a shows that high PM_{10} concentrations occurred in the evening hours (between 18:00 and 21:00) at the Frontage Site when the winds were coming from the south southwest. A close view of this figure in conjunction with Figure 12a reveals that the high PM_{10} concentration at this site occurs at low wind speeds in the evening. Figure 13a shows that PM_{10} concentration at this near-road site peaked in the evening and maintained reasonable high concentrations into the nighttime as well as in the early morning hours. Figure 13b shows similar observations for $PM_{2.5}$ at this location. Near-road NO_2 concentrations appeared to be less influenced by the wind direction, as seen in the figure that high concentrations were observed in the evening hours under southernly and westerly winds. NO_2 concentrations were at the lowest levels between midday and sundown. Highest O_3 concentrations took place in the midday hours when the temperature was highest during a day, as seen in Figure 13d. Interestingly, high O_3 concentrations occurred when the winds were coming from downtown (or the northeast direction) even at higher wind speeds (Figure 12d). This provides further evidence that O_3 pollution is more ubiquitous in the city and less influenced by the local traffic emissions.

Figure 14 shows the same time varying concentration plots for the Residential Site. The time of day and wind direction for the occurrence of peak concentration at this site is similar to that observed at the Frontage Site for each TRAP. High PM_{10} and $PM_{2.5}$ occurred in the evening hours when winds were coming from I-10 to the south. Pollutant concentrations observed at the state-operated site (Reference Site) are also presented in Figure 15. High PM concentrations are not seen to come from the south, as the site is located away from I-10 in a different geographic setting. The times of occurrence for high NO_2 and O_3 concentrations are consistent with those observed at the Frontage and Residential Sites but the impacts of wind direction on the levels of pollution are no longer the same.

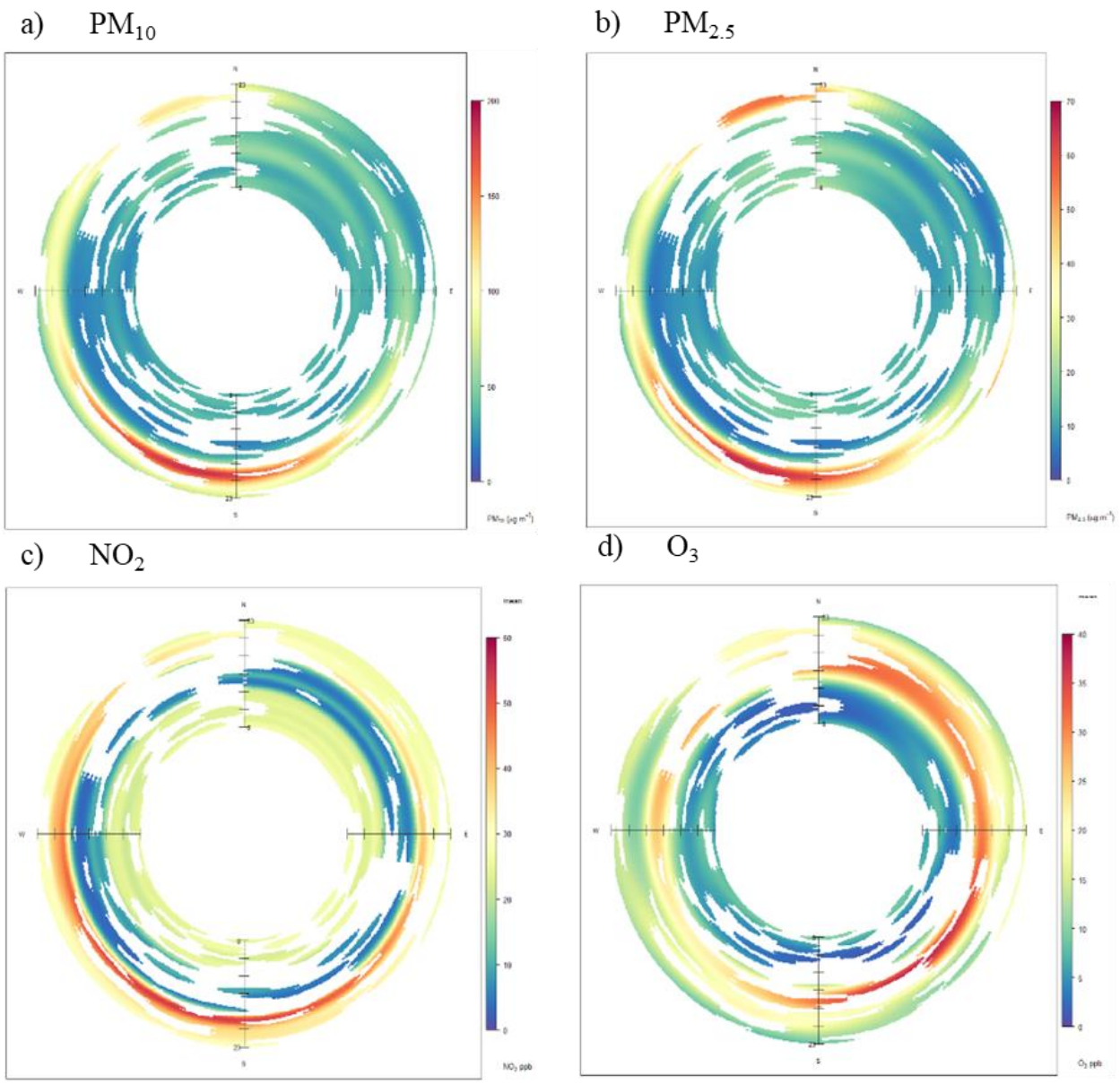

Figure 13 Time Varying Concentration Plots for the Frontage Site a)PM_{10}, b) $PM_{2.5}$, c) NO_2 and d) O_3

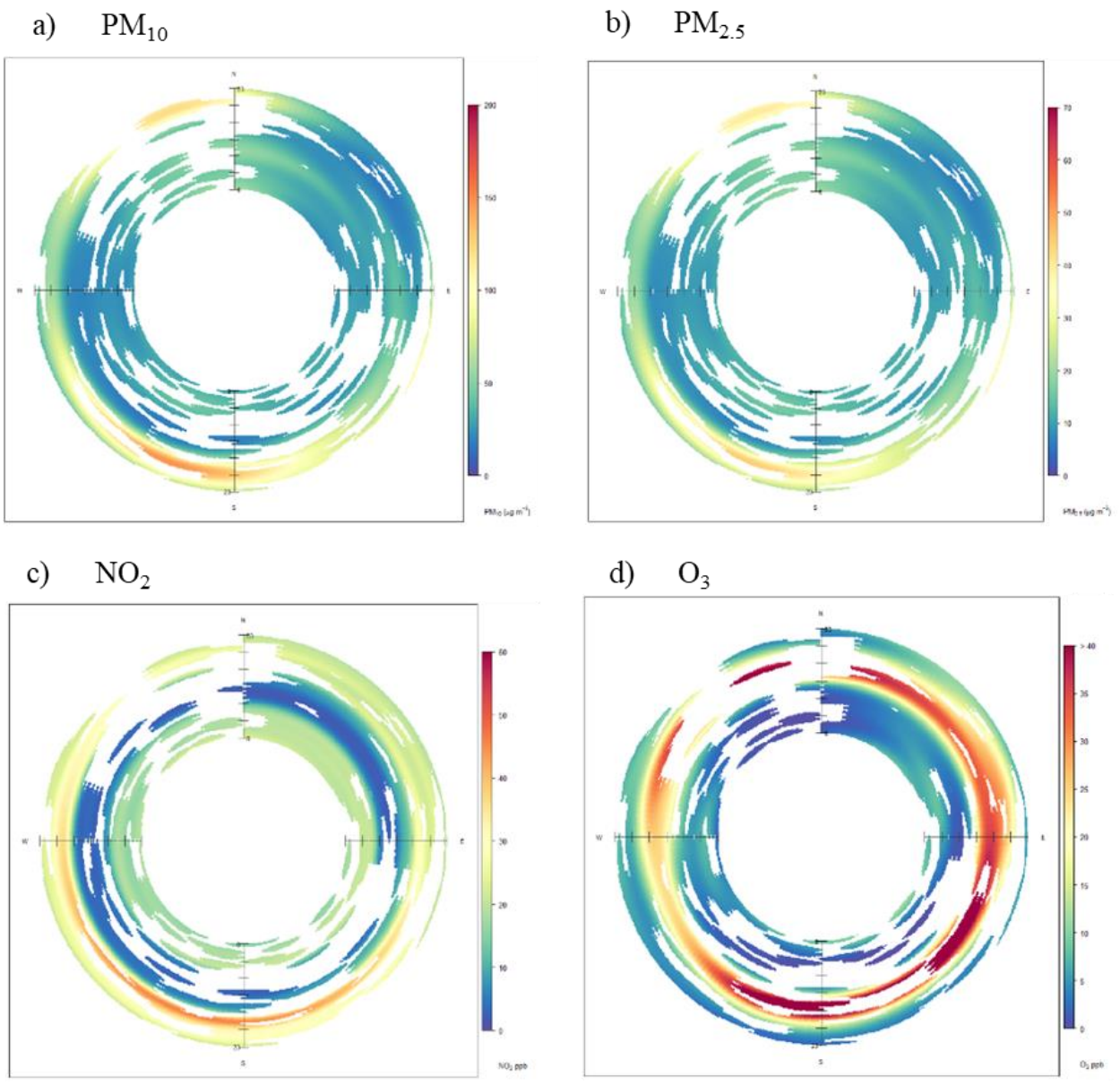

Figure 14 Time Varying Concentration Plots for the Residential Site a)PM_{10}, b) $PM_{2.5}$, c) NO_2 and d) O_3

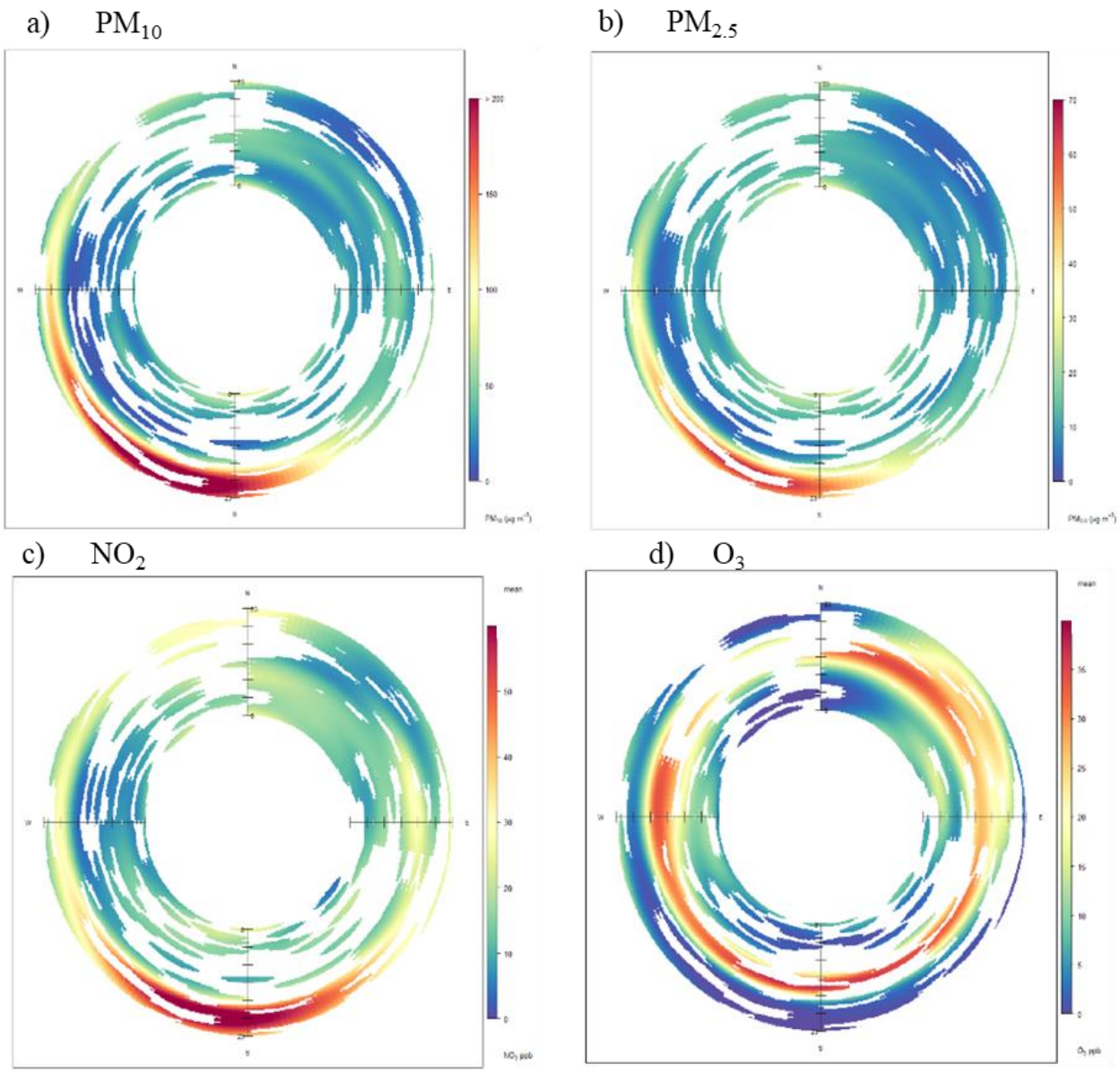

Figure 15 Time Varying Concentration Plots for the Reference Site (CAMS 41) a)PM_{10}, b) $PM_{2.5}$, c) NO_2 and d) O_3

3.2.4 Comparison of Stationary Site Measurements

Hourly pollutant values at the Frontage and Residential Sites were further analyzed and compared to the reference site CAMS 41 located approximately 4 km east of the study area. Figure 16 shows the time-series plots for all pollutant concentrations collected during the study. PM concentrations measured at all three locations peaked at the same times. In general, NO_2 values at both testing sites follow a similar pattern to the values collected at CAMS 41, although the Frontage Site showing a few peaks higher than those reported at both CAMS 41 and the Residential

Site. As is expected with the ubiquity of O_3, ozone concentrations observed at CAMS 41 and the two near-road sites follow the same trend and are almost identical during the two-week period monitored. Figure 17 – Figure 19 are the Pearson Correlation plots between the stationary sites of the hourly averaged data. R^2 values are generally higher between the Frontage and Residential Sites than between them and the Reference location. This likely has to do with the distance between sites, Frontage and Residential are about 400 m apart while the reference site is about 4 km from them. Among the air pollutants O_3 has the highest correlation between all three sites, suggesting its potency as a background pollutant.

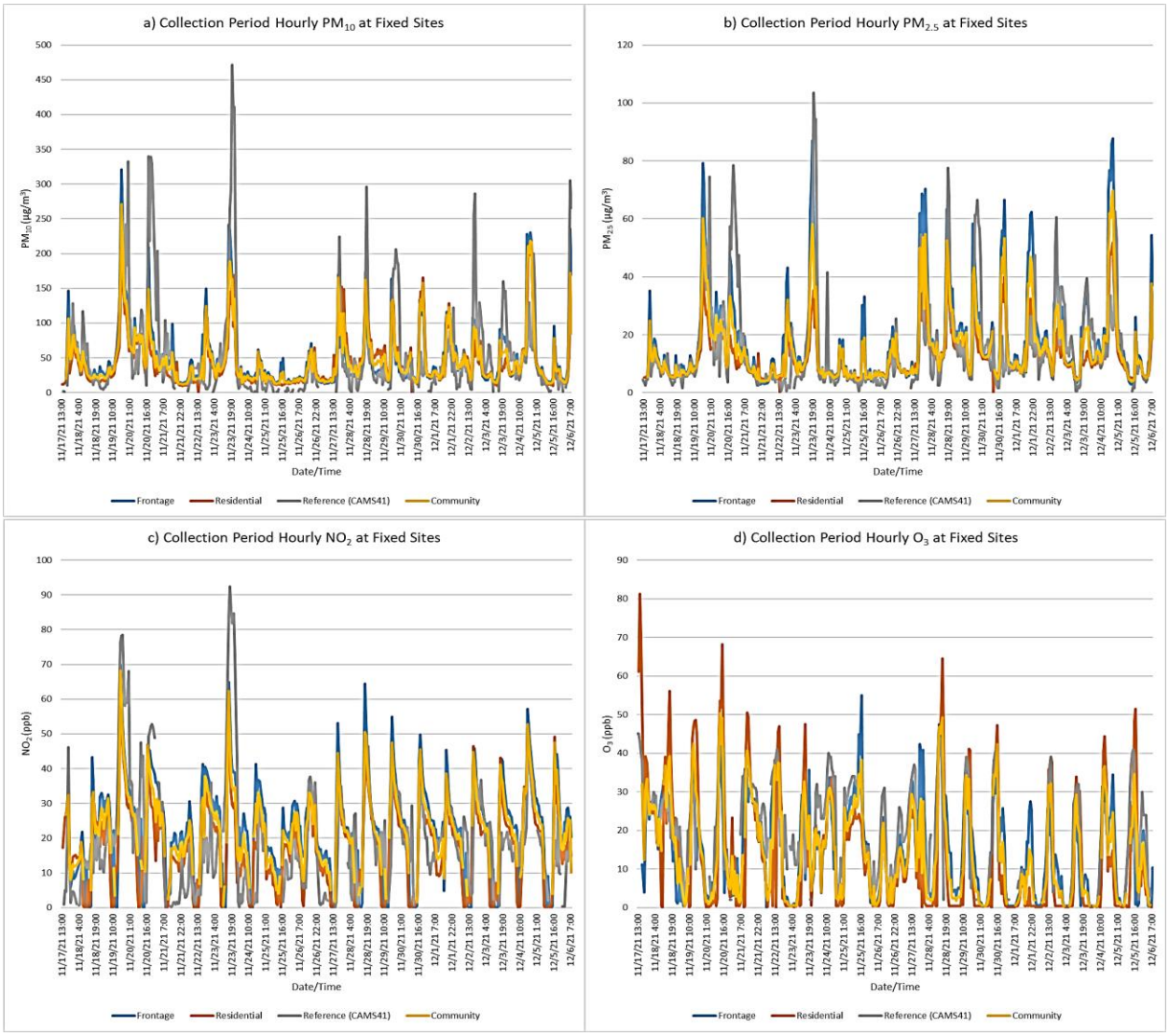

Figure 16 Comparison of Hourly pollutant data observed at Frontage, Residential and CAMS 41 a) PM_{10}, b) $PM_{2.5}$, c) NO_2 and d) O_3 data

Figure 17 Pearson Correlations between Frontage and Residential, 1-hour a)PM_{10}, b) $PM_{2.5}$, c) NO_2 and d) O_3

Figure 18 Pearson Correlations between Frontage and Reference, 1-hour a)PM_{10}, b) $PM_{2.5}$, c) NO_2 and d) O_3

Figure 19 Pearson Correlations between Residential and Reference, 1-hour a)PM_{10}, b) $PM_{2.5}$, c) NO_2 and d) O_3

3.2.5 Comparison of On-Road and Stationary Site Measurements

Since the on-road monitor passed by the near-road sites for only a few seconds at a time, and near-road sites recorded data by 5-minute averaging, all the instances of the on-road measurements by the near-road site during those 5 minutes were processed as the "on-road 5-minute average" for that specific 5 minutes. The "on-road 5-minute averages" collected in the same hour near the near-road location were then aggregated into an "on-road hourly average". In a way, the on-road 5-minute average may have only a few seconds of concurrent observations whereas the "on-road hourly average" are likely to have 3 to 4 times more seconds of data than the "on-road 5-minute average" spreading in an hour when the concurrent near-road hourly average was collected.

Hourly Concentrations

On-road measurements were compared to the near-road measurements observed at the two sites along the route. It is observed that in general on-road measurements show strong relationships with fixed site observations. Figure 20 shows on-road measurements compared to near-road measurements at the Frontage Site and Residential Site. Each point represents one hour of data and break lines are inserted to show the separation of days. As discussed previously, the near-road site, Frontage Site, is approximately 13 m from the road and 15 m above the interstate; the Residential Site was located approximately 10 m from the road and 5 m above.

Figure 20 shows that the trend of on-road hourly average of PM_{10} agrees very well with that of the near-road measurement immediately adjacent to I-10 at the Frontage Site or in the residential neighborhood at the Residential Site, although the magnitudes of on-road PM concentrations tend to be lower than those reported for the near-road sites. Similar trend is observed in the same figure for $PM_{2.5}$. However, the underestimation is more pronounced at higher PM_{10} than $PM_{2.5}$ (circled in blue in Figure 20) when higher winds were present on that day. Because the size of PM emitted from transportation activities are dominated by fine particulate (i.e., $PM_{2.5}$) and on-road vehicles are constantly submerged in the wake generated by vehicle movements, PM_{10} that is primarily associated with regional background geologic or fugitive emission sources would be less likely to impinge on the moving vehicle. As a consequence, PM_{10} observed by a moving vehicle is expected to be less than that observed at a fixed station (either Frontage or Residential) which is approximately 15 m above the road surface. Pollutants with no

geologic or fugitive association such as $PM_{2.5}$, O_3, or NO_2, on the other hand, do not demonstrate the same behavior or actually behave in the reverse direction (circled in red in Figure 20). Indeed, on-road measurements of NO_2 varied greatly and were higher than those measured at the near-road measurements. On-road measurements for O_3 were almost identical to near-road measurements at both sites. As established by other analyses in this study, O_3 is greatly ubiquitous in the area and only varies diurnally.

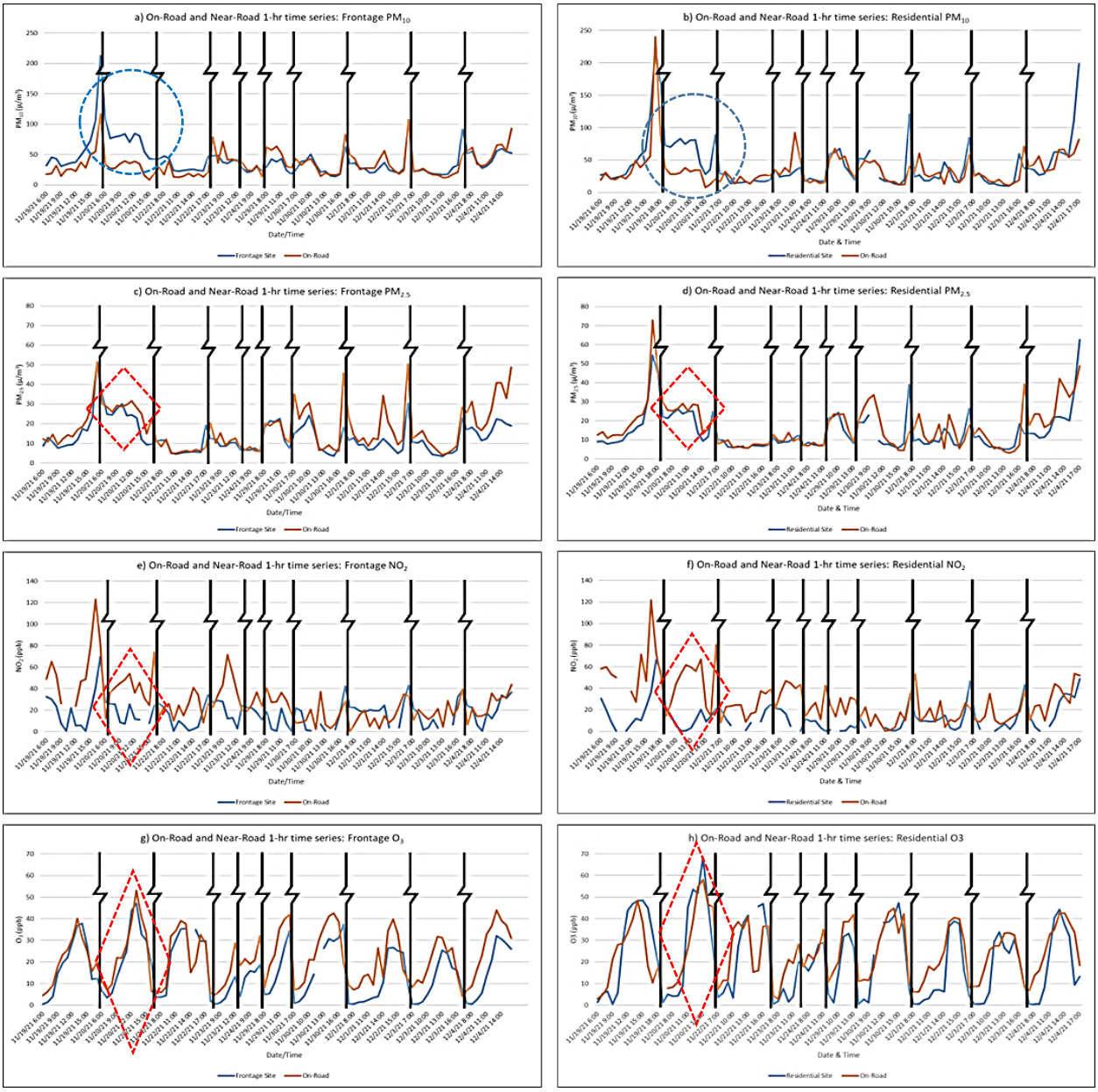

Figure 20 Comparison of Hourly pollutant data observed at Frontage, Residential sites and On-road data (1 Hour)

Five-Minute Pollutant Concentrations

Figure 21 shows time-series plots of the 5-minute averaged pollutant data observed at the two near-road and on-road sites. Break lines are omitted in the figure since there are too many of these 5-minute averages. Five-minute averaging comparison is expected to have higher performance over 1-hr comparison since the magnitude of the fluctuation in concentration within 5 minutes should not be as significant as in an hour. It is seen in the figure similar trends exist for all pollutants, except NO_2. Figure 22 shows the associations between the paired on-road and near-road data at the Frontage Site, using 5-minute averages. Figure 23 shows the associations between the paired on-road and near-road data at the Residential Site, using 5-minute averages. The associations between near-road and on-road concentrations continue to be strong for $PM_{2.5}$ and O_3 in comparison to the 1-hr averages (R^2 = 0.55 vs. 0.71, and 0.73 vs. 0.73, respectively) at the Frontage Site, moderate for the Residential Site (R^2 = 0.58 vs. 0.68, and 0.54 vs. 0.66, respectively). As previously observed, $PM_{2.5}$ and O_3 concentrations continue to show weak to no associations at both Frontage and Residential Sites.

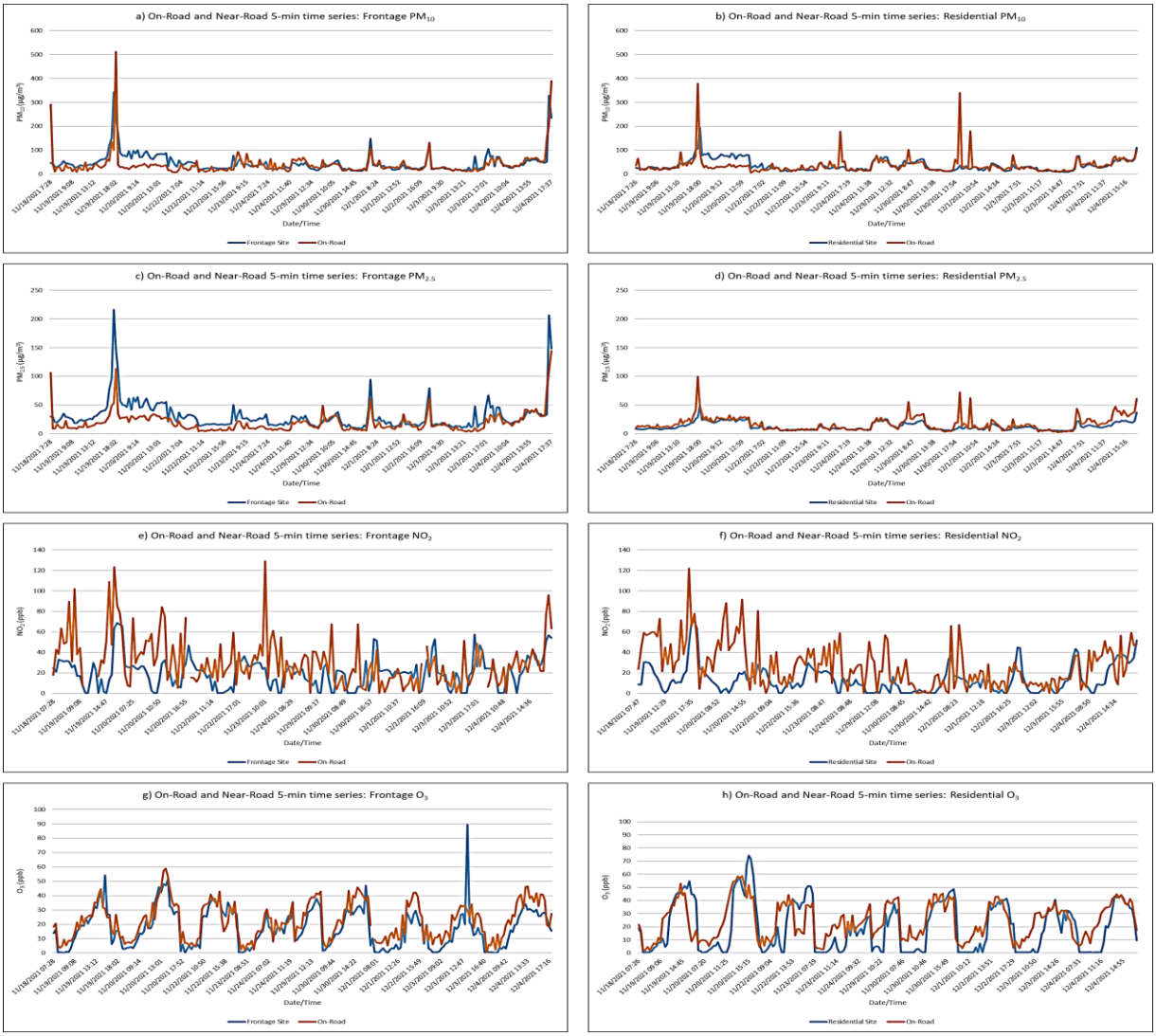

Figure 21 Comparison of 5-minute pollutant data observed at Frontage, Residential Sites and On-road data

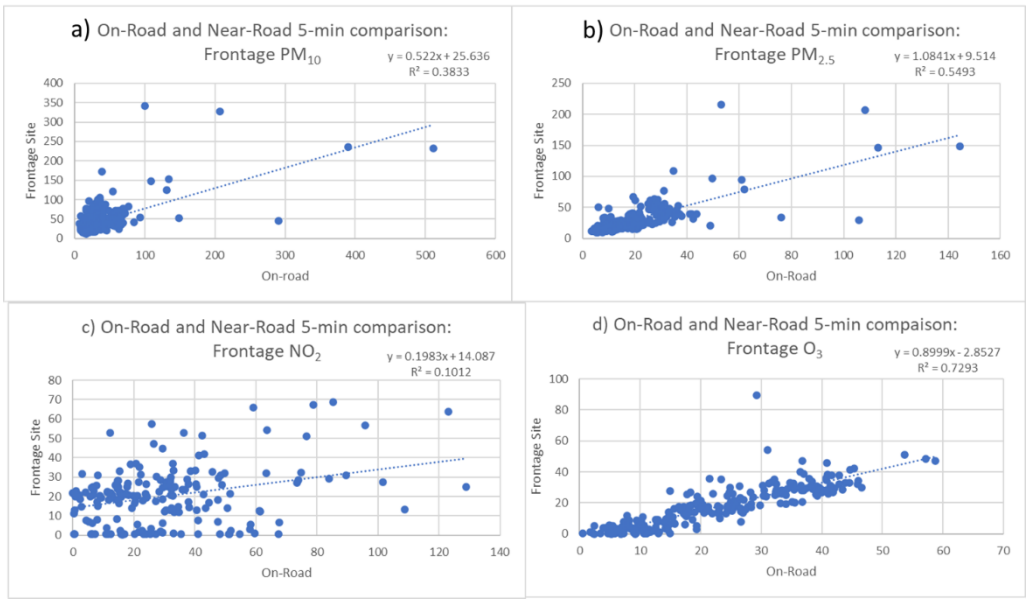

Figure 22 Pearson Correlations between On-road and Near-road (Frontage), 5-minute a)PM_{10}, b) $PM_{2.5}$, c) NO_2 and d) O_3

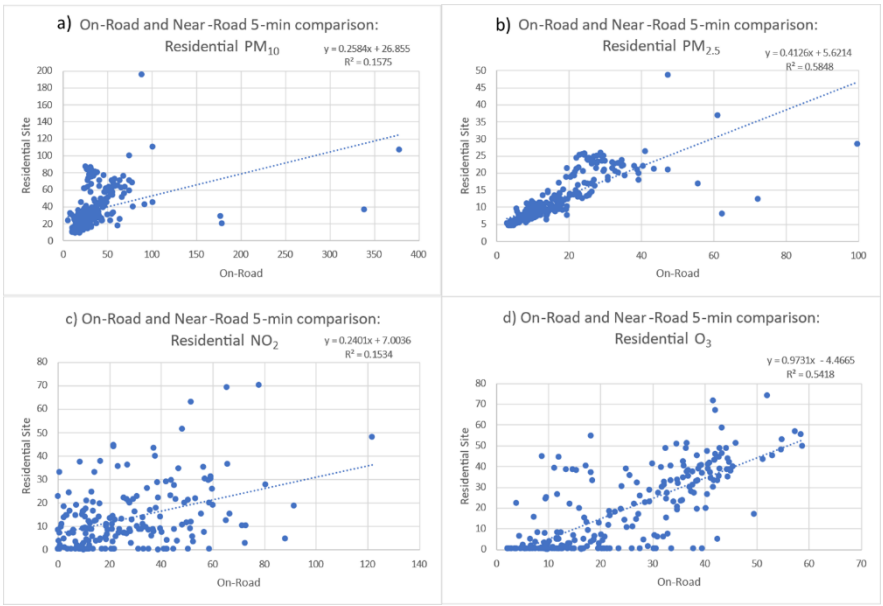

Figure 23 Pearson Correlations Between On-road and Near-road (Residential), 5-minute a)PM_{10}, b) $PM_{2.5}$, c) NO_2 and d) O_3

CHAPTER 4: DISCUSSION

4.1 Spatial averaging near a stationary site

In the current study, each trip took approximately 20 minutes and resulted in approximately 5 seconds of data (or 5 data points) of pollutant concentration in an hour for making a "pseudo collocated" comparison between the hourly averaged data measured at a stationary site and the on-road data recorded by the on-road monitor passing the site. Figure 24a shows the road segment used in the analysis for the Residential site. Figure 24b shows the segment used in developing a spatially averaged 1-hour pollutant concentration for comparison with the Frontage Site.

a) Spatially averaged points to compare on-road to near-road monitoring (Residential Site)

b) Spatially averaged points to compare on-road to near-road monitoring (Frontage Site)

Figure 24 Spatial data points used for estimating hourly average on-road concentration near a stationary site, a) Sunbowl and b) CAMS 12

The hourly on-road and stationary pollution data appear to agree very well with each other for all TRAPs in the two less travelled streets. Figure 20 shows that the magnitudes and the trends of the on-road PM data (both PM_{10} and $PM_{2.5}$) resemble closely with each other at the near-road sties. For a more ubiquitous TRAP such as O_3, the agreement is extremely well (Figure 20). NO_2 data observed by the on-road monitor show higher values than those observed at a roadside stationary site. On-road NO_2 concentrations are strongly affected by local meteorology, photolysis

of NO_2 and O_3, solar radiation, and tailpipe emissions from various types of vehicles. The immediate, complicated photochemical reactions of NOx at tailpipe might have contributed to the incongruity between the on-road and near-road stationary data. Nevertheless, the hourly averaged NO_2 on-road data follow a similar trend and peaks concurrently as that observed at this site.

One notices that our mobile monitoring on the frontage road may not be a good representation of the on-road pollution on the interstate highway. Pollutant concentrations on the interstate highway could be 50% higher than those measured on the frontage road [29]. Baldauf et al [29] reported that CO, NO_2, BC, and UFP concentrations on highway were ~50% higher than those measured within 50 m off the edge of the highway and the TRAP concentrations decrease more gently after the initial 50 m off the highway. The magnitudes of the TRAP concentrations along the highway are highly variable depending on the vehicle activities, fleet composition, local emission sources, and meteorological conditions. Our on-road data were collected on frontage road that is 10-20 m off the interstate highway and could experience a significant reduction. The concentration gradients from the frontage road to the Frontage Site, which is further away from the interstate highway, is expected to be flatter, resulting a better agreement between the on-road and near-road TRAP concentrations.

4.2 Comparison of Near-road to On-road Pollutant Concentrations

Table 3 summarizes the average pollutant concentrations collected from the near-road and on-road monitors. On-road data represent the averages of data collected when the on-road monitor passed within 25 m of the fixed sites in an hour.

Table 3 Summary of On-Road and Near-road pollutant data at Fixed Locations

Pollutant	On-Road	Frontage	$\frac{\text{On-Road} - \text{Frontage}}{\text{On-Road}}*100$	On-Road	Residential	$\frac{\text{On-Road-Residential}}{\text{On-Road}}*100$
$PM_{2.5}$ ($\mu g/m^3$)	18.9	14.4	23.8%	17.4	13.1	24.7%
NO_2 (ppb)	29.0	18.0	37.9%	29.0	13.3	54.1%
O_3 (ppb)	22.0	17.2	21.8%	24.4	20.5	16.0%
PM_{10} ($\mu g/m^3$)	34.5	46.9	-35.9%	35.3	37.9	-7.4%

For a near-road location immediately adjacent to a busy interstate highway such as the Frontage Site, primary on-road traffic-related pollutants such as $PM_{2.5}$, NO_2, and O_3 would exhibit higher concentrations than those observed at near-road locations, as seen in the 2nd and 3rd columns of Table 3. The concentration gradients (or decreases in concentrations) from the frontage road to near-road location for primary TRAP ($PM_{2.5}$, NO_2, and O_3) vary between 20 to 40 % which are in line with the results reported in a study conducted in Phoenix, AZ [29]. The decreases in concentrations in the residential community with less travelled streets appear to be much flatter (~20%) except for NO_2 (last column of Table 3). As previously discussed, the complex chemical and photochemical reactions at the vehicle exhausts increases the variability of on-road NO_2 concentrations and its dispersion to the near-road environment.

PM_{10} concentrations display a pattern very different from that for the other 3 pollutants. PM_{10} in El Paso as well as in many other southwestern cities in the U.S. is primarily emitted from unpaved roads or dry arid surfaces and the impact on air quality is more regional than local. It is understood that the vehicle induced turbulence behind and around the moving vehicles on highway may shield the on-road monitors from PM_{10} carried by the regional winds. Consequently, we observed higher PM_{10} concentrations at near-road site than on-road, as displayed in the 2nd and 3rd columns in Table 3. In the residential community away from the highway and with less traffic, PM_{10} is expected to be dominated by the regional sources with little impact from the less travelled streets. Indeed, we observed little variation between the near-road and on-road PM_{10} concentration (Columns 5 and 6 of Table 3). The elevation difference between the Residential Site and the on-road monitor might be the primary attributor for the small 7% increase in PM_{10} concentration from on-road to near-road in this residential community. Furthermore, it is observed in Table 3 that the on-road concentrations on the residential street for $PM_{2.5}$, NO_2, and O_3 remain almost the same as those observed on the frontage road, implying that the on-road concentrations on the frontage road are similar to those in the near-road community and is another indication of flatter concentration gradients off the highway. Table 3 shows that TRAP concentrations decrease from frontage road adjacent to I-10 to near-road by 24% for $PM_{2.5}$, 22% for O_3, and 38% for NO_2 while PM_{10} increase by 36%. Similar trends were observed in the community where the on-road PM concentrations decreases by 25% to near-road, 54% for NO_2, 16% for O_3, and decreases by 8.4% for PM_{10}.

4.3 Using Data Observed from On-road Monitors for Community Exposure

In many air epidemiological studies, pollutant concentrations measured at a centralized location are commonly used to represent the exposure concentrations for the studied population regardless of the spatial and temporal variabilities caused by factors such as topology, meteorology, traffic conditions, and locations of emission sources. Representativeness of the data collected from a central fixed location as the exposure concentrations has been the primary sources of error in many health effect studies. The on-road monitor has the advantage of collecting spatiotemporal pollution data that may be a better representation of the true exposure concentrations, as described below:

A true space-time average for a studied area $C_{t,s}$ will be the average concentrations measured at location i and time t, where i = 1, N and t = 1, M

$$C_{t,s} = \frac{1}{M \cdot N} \sum_{i=1}^{N} \quad \sum_{j=1}^{M} C(x_i, t_j) \,,$$

while a space averaged concentration at a given time t_o is C_s

$$C_s = \frac{1}{N} \sum_{i=1}^{N} C(x_i, t_o),$$

a time averaged concentration at a given central, fixed location is C_t, and

$$C_t = \frac{1}{N} \sum_{j=1}^{N} C(x_o, t_j)$$

an on-road space-time averaged concentration $\widetilde{C_{t,s}}$ is

$$\widetilde{C_{t,s}} = \frac{1}{N} \sum_{j=1}^{N} C(x_j, t_{j+1})$$

It can be easily seen in the above expression that as N$\rightarrow \infty$, only $\widetilde{C_{t,s}} \rightarrow C_{t,s}$. In a way, no matter how many samples collected at a fixed location or no matter how many samples collected from different locations at a given time can correctly represent a true space-time average. Only the data collected by an on-road monitor in the study domain can adequately represent the true space-time average providing a large number of samples are collected.

Figure 25 shows the distribution of the observed hourly data collected at each individual site and by the on-road monitors. The middle line represents the median, the box the 25th and 75th percentiles, and the whiskers the 5th and 95th percentiles (or Mean±1.5 IQR). Mean± SD is

included in the box. The concentrations observed at the Frontage and Residential Sites are averaged and listed as "Community" concentrations in Table 4 for comparison with data recorded at a nearby TCEQ community exposure site, as displayed under "Reference (CAMS41)". Only the hourly data concurrent to the study period are used in this table.

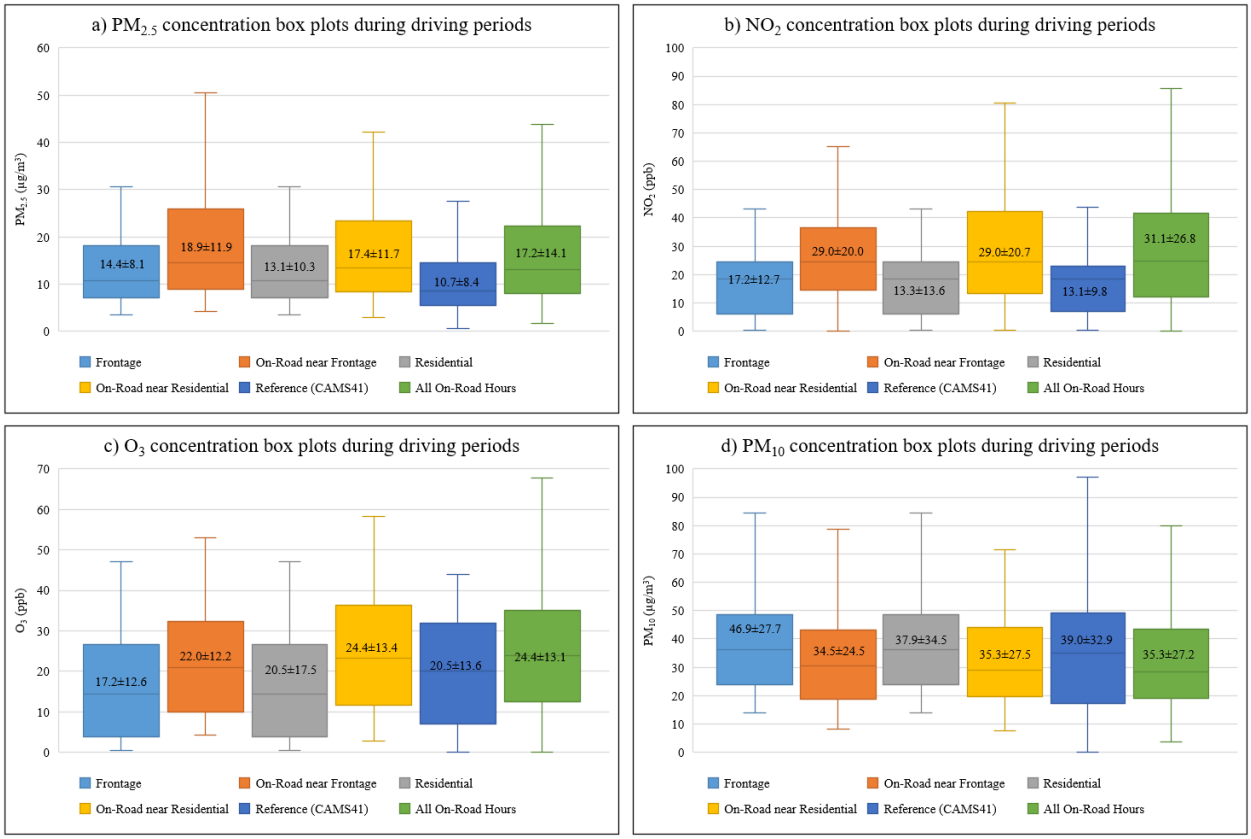

Figure 25 Box plots of collected data during driving hours of on-road data, Frontage, Residential, and Reference a) PM_{10}, b) $PM_{2.5}$, c) NO_2 and d) O_3

Table 4 Comparison of On-road, Community, and Reference Site: Total Pollutant data and Percent Difference

Pollutant	On-Road	Reference (CAMS41)	Community	$\frac{\text{On-Road} - \text{Community}}{\text{On-Road}} * 100$
$PM_{2.5}$ (µg/m^3)	17.2	10.7	13.8	20.1%
NO_2 (ppb)	31.1	13.1	15.7	49.7%
O_3 (ppb)	24.0	19.4	18.9	21.5%
PM_{10} (µg/m^3)	35.2	39.0	42.4	-20.5%

Table 4 shows that the average concentrations from the two community monitors (Column 4, Table 4) approach the observations at the centralized site (Column 3, Table 3) whereas the on-road monitor reported data that are in line (within ±20%) with the Community averages for all TRAPs except NO_2. It is not possible to determine which data would best represent the average community exposure concentrations without a more detailed study. Nevertheless, we believe the mobile data could be a better presentation for community exposure concentrations if a sufficiently large number of trips were taken.

4.4 Spatial Distribution of TRAPs in the Roadside Community

Continuous hourly TRAP data collected at the two near-road sites are compared to the Reference Site in Figure 26 to assess the spatial concentration variations in this roadside community. Figure 26 shows the hourly concentration distribution at the 3 locations for 14 full days. It can be seen in the figure that the TRAP concentrations near a busy highway at the frontage road were higher than the respective concentrations observed in the community 500 m off the busy highway, based on the mean and median values. TRAP concentrations observed at the Reference site appear to be in good agreement with those observed in the near-road community (15.5 vs 18.1 and 12.1 for $PM_{2.5}$; 20.0 vs. 23.8 and 19.1 for NO_2; 14.9 vs. 14.4 and 14.2 for O_3; 57.2 vs. 51.2 and 43.5 for PM_{10}). However, the distributions could be quite different in terms of median and SD for the distribution which implying potential inhomogeneous distribution of concentrations in a roadside community and the inadequacy of using a centralized station for community monitoring.

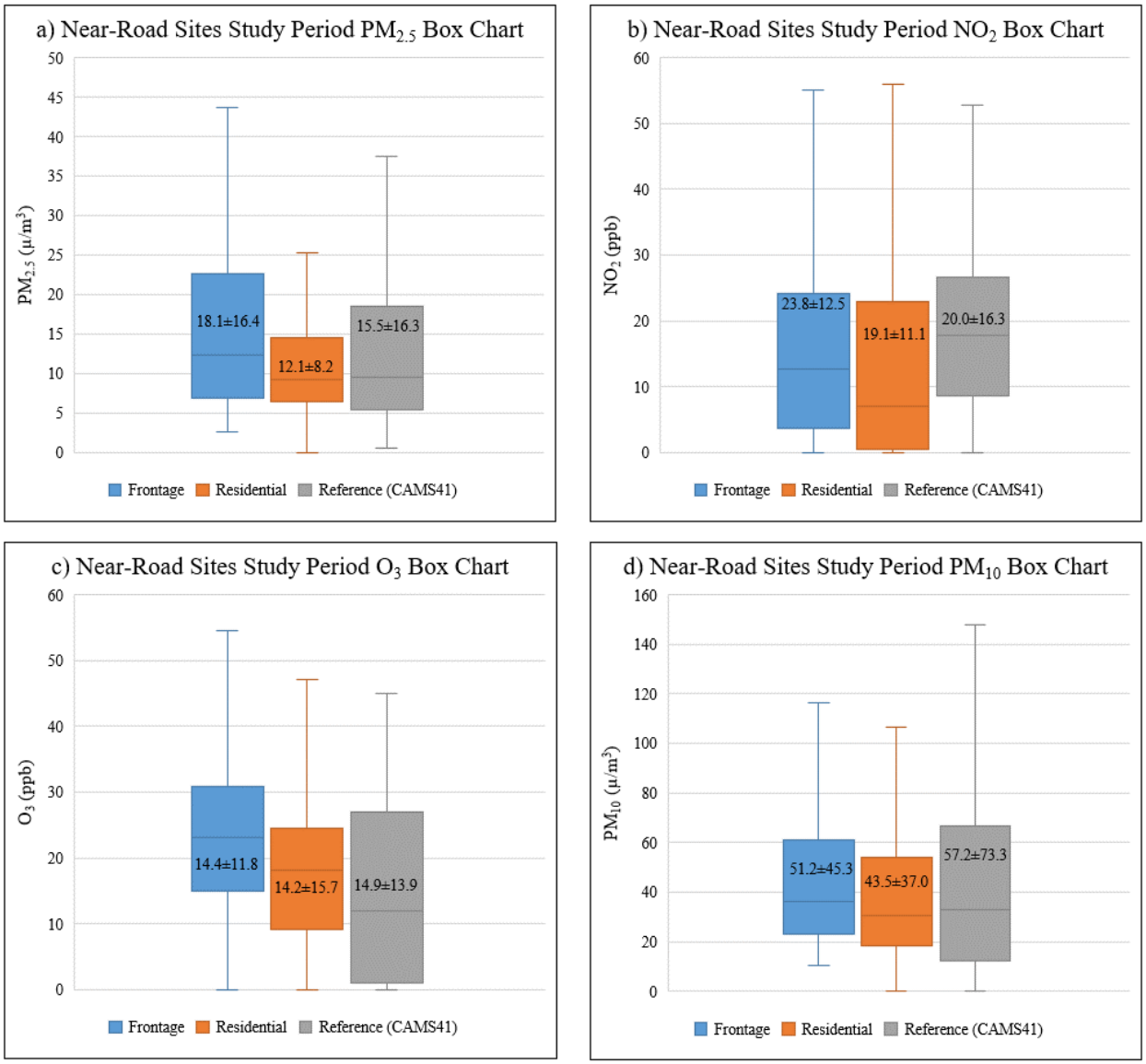

Figure 26 Box plot of collection period data at Frontage and Residential a) PM_{10}, b) $PM_{2.5}$, c) NO_2 and d) O_3

Figure 27 shows the daily average of the on-road pollutant concentrations plotted on a 3D scatterplot, with x and y axes being Latitude and Longitude, respectively. This figure includes days as the z-axis. Each loop in the figure represents the average TRAP concentrations in a given day. Each loop in Figure 27 can be further dissected to the hourly average concentrations occurred in the same day. Figure 28 shows, as an example, the hourly average of on-road pollutant concentrations on a high day during the study period, 11/22/2021. The z-axis in this figure indicates the hour of the day. PM values showed higher concentrations occurred at stops and intersections along the route, independent of hour of day. However, $PM_{2.5}$ showed peaks during early hours and near I-10 (southeast view of figure, circled in red). O_3 showed the greatest evidence of a diurnal pattern throughout the day. O_3 concentrations are consistent along the route and only vary with each hour difference. The 1-hr average concentration loop shown in Figure 28 represents the average concentrations of the 3 trips along the same route collected during the hour. Figure 29 shows the 1 hour on-road pollutant concentrations during the 3pm hour of 11/22/2021. PM_{10} and $PM_{2.5}$ are the most consistent along the route while NO_2 and O_3 vary highly throughout the 3 runs, suggesting a temporal rather than spatial pattern. Difference in concentrations among different trips can be visualized in the figure. Figure 27 through Figure 29 show that the spatio-temporal variation of TRAP concentrations in a near-road community. As stated in the previous section, exposure concentrations collected from a central fixed location could never represent the true concentration averages over the space and time domain of the community. Only the on-road monitor has the advantage of collecting spatiotemporal pollution data that are a better representation of the true exposure concentrations.

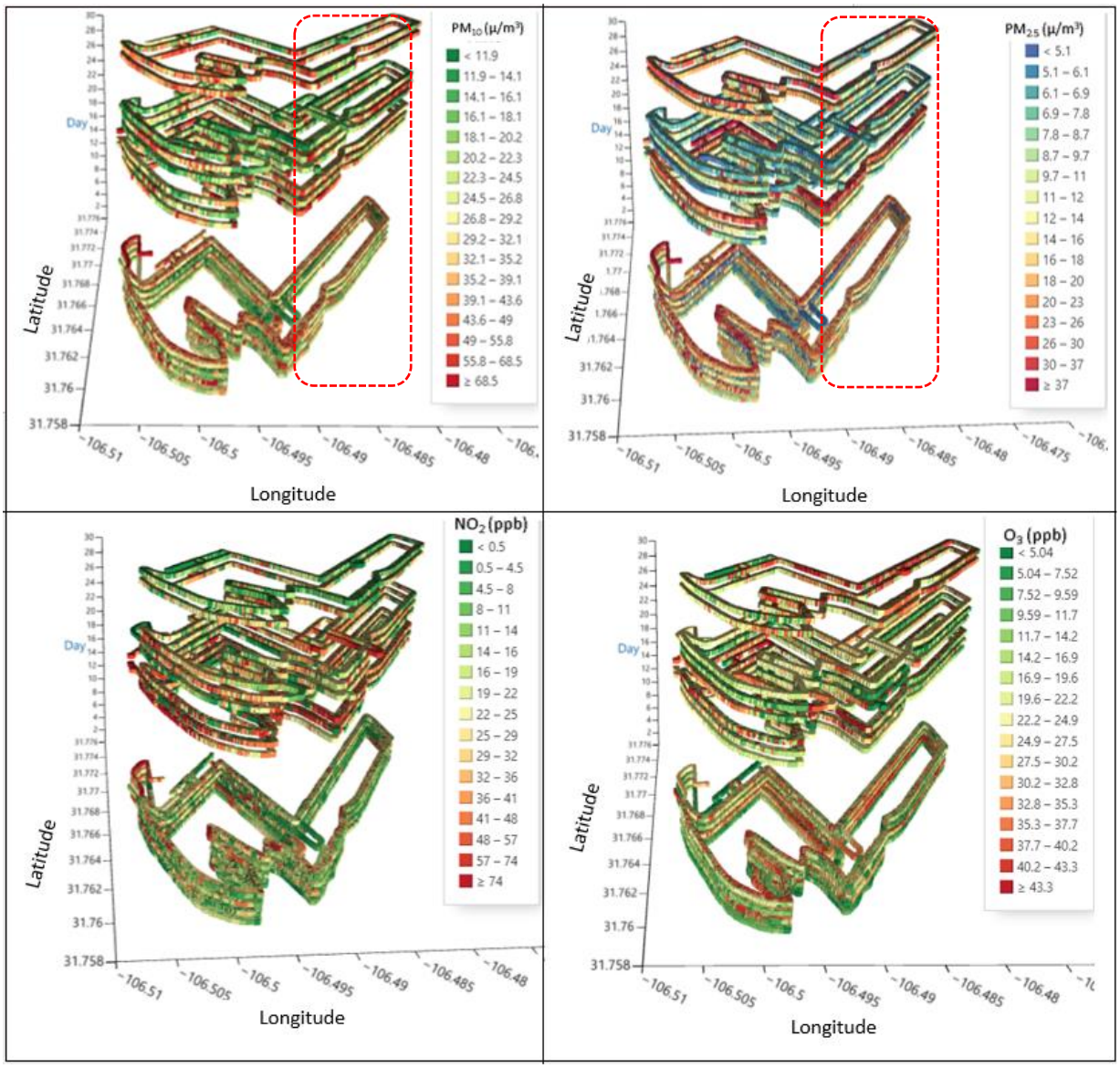

Figure 27 Daily average of On-Road Pollutant Concentrations

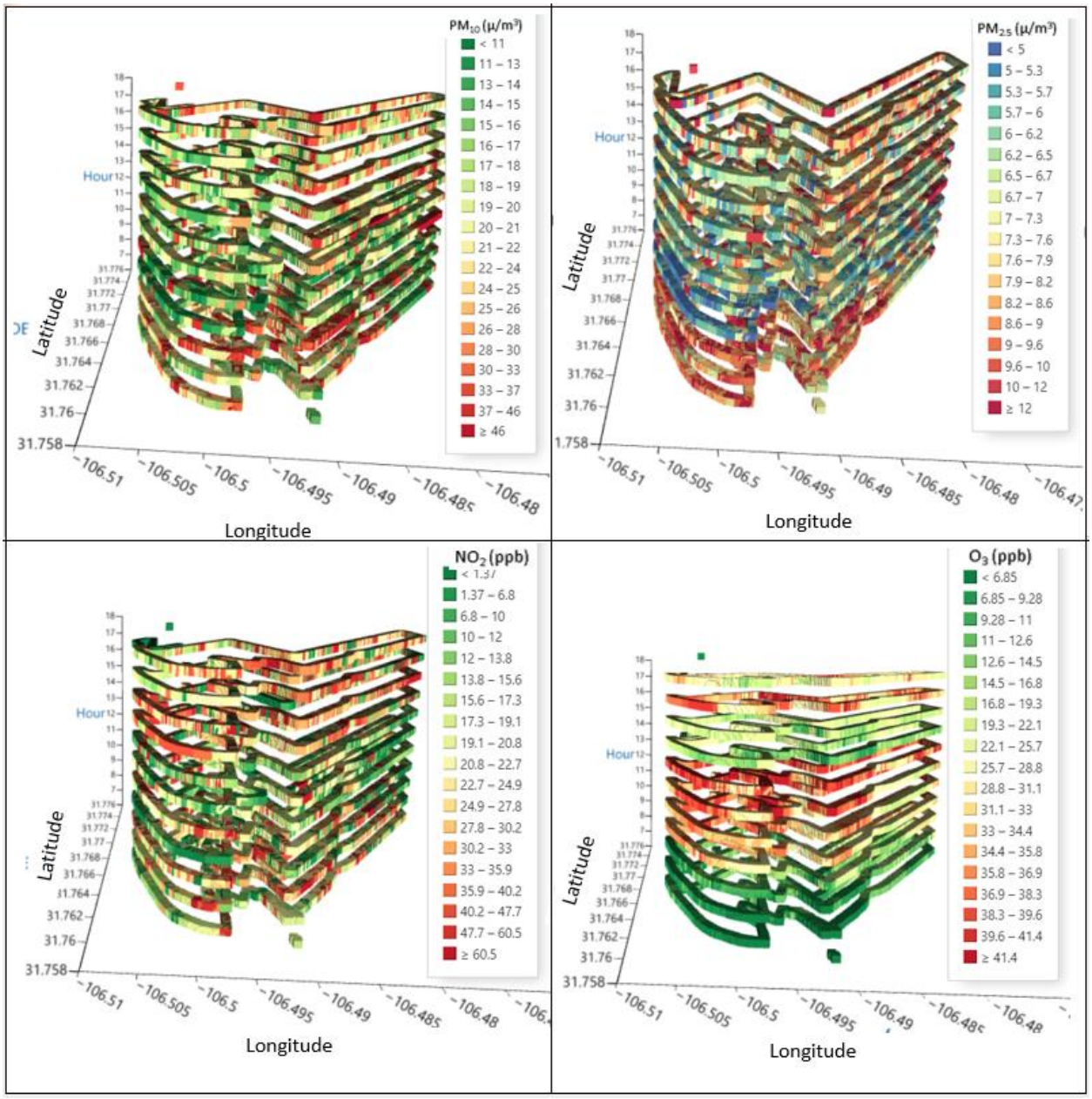

Figure 28 Hourly Average of On-Road Pollutant Concentrations, 1 day (11/22/2021)

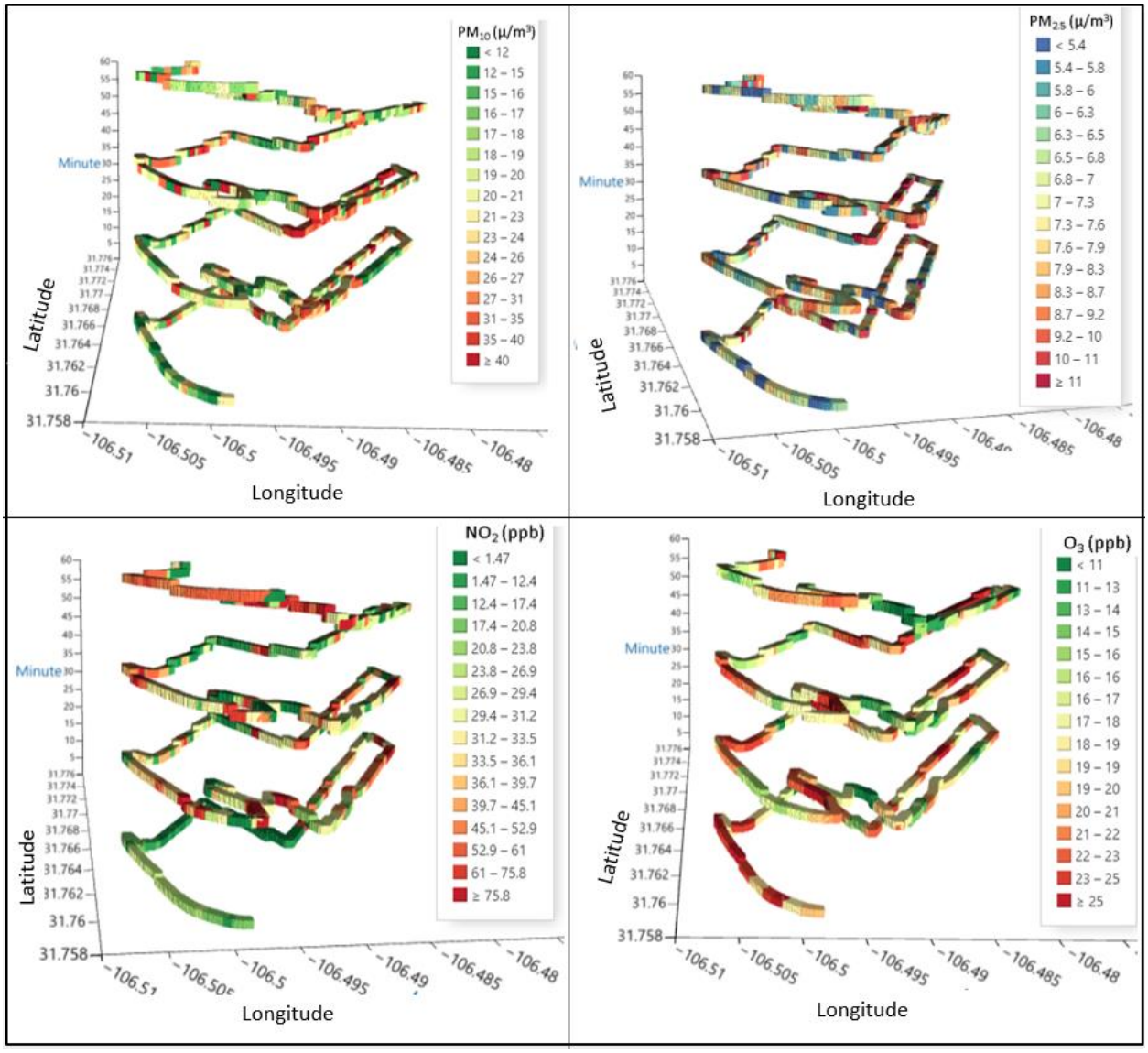

Figure 29 1 hour On-Road Pollutant Concentrations for one hour (3pm, 11/22/2021)

4.2 Limitations and applications

Concurrent on-road and stationary monitoring of TRAPs using respective EPA FEM-designated instruments and a GPS tracking device equipped in the vehicle to provide real-time data of pollutant concentrations, coordinates of on-road measurements, and vehicle speed is demonstrated in this study. The corresponding spatial resolution for each measured pollutant concentration depends on the averaging time of the monitor and the vehicle speed. In this study, the minimum averaging times for PM, NO_2, and O_3 monitors are 6, 5, and 10 seconds, resulting in minimum spatial averages of approximately 60-m, 100-m, and 50-m for each of the recorded on-

road concentration data, respectively. The 1-second average concentrations between two consecutive recorded readings were calculated by interpolation to yield concentration data representing a spatial average of approximately 10-m. The algorithm used in the interpolation would result in various degree of data smoothing and would also prevent the monitors from detecting the spatial variation within the minimum detection zone. A fast response device would help eliminate this deficiency, particularly if measurements are expected to take place on highways with higher speed limit.

The current study was conducted in a low traffic community where traffic conditions were significantly different from other places and other times. The vehicle speed was kept at 30 mph or lower under good traffic conditions. It is encouraging to observe that on-road monitoring provides data that are well correlated to the data monitored at a stationary road-side monitor, whether the on-road data included only a few points per hour or per 5-minute for comparison. On-road data may well represent the community exposure in a neighborhood where traffic emissions are less affected by the traffic and road conditions and where point sources are non-existing. These circumstances would need to be addressed especially if a general guideline for on-road monitoring were to be developed. The advantages, however, are also coupled with disadvantages of not being able to record simultaneous observations at multiple locations and not being able to report sufficient data at a stationary location for exposure and health outcome assessments. A well designed on-road monitoring campaign could provide sufficient data points and result in more realistic exposure concentrations in an area where community exposure could not be represented by the data collected from a single station (e.g., a community in complex terrain, various transportation facilities, complex background emission sources). Our study demonstrates that on-road air monitoring in a less travelled community can correctly detect the exposure concentrations that are representative of the community as well as near-road receptors.

CHAPTER 5: SUMMARY AND RECOMMENDATIONS

While efforts have been made to promote transit, walking, and bicycling and other non-motorized transportation modes as a healthy lifestyle, the exposure of human to pollutants while carrying out these activities is yet to be fully understood. This project evaluated the feasibility of using transit vehicles traveling on fixed routes for near-road exposure assessment. Continuous on-road measurements of four TRAP pollutants (PM_{10}, $PM_{2.5}$, NO_2, and O_3) were recorded in conjunction with GPS locations. Concurrent near-road measurements at two project-established stationary sites as well as a state-operated site monitoring data of the same pollutants were used to verify and provide associations with the on-road data. The data could be used to quantify exposures experienced by pedestrians, passengers, bus users, and near-road residents.

One objective of this study was to assess the appropriateness of using the spatio-temporal on-road air monitoring data for representing community exposures to TRAPs. This was done through the evaluation of on-road data collected on frontage road and in a residential community against data collected from two roadside locations and one EPA approved state-operated ambient air monitoring site. We have found that while TRAP concentrations observed at a central site appear to be in good agreement with those observed in the near-road community, potential inhomogeneous distribution of concentrations in a roadside community may be better represented by a sufficient number of spatio-temporal data in the community generated by an on-road monitor.

Our second objective of assessing the feasibility of using on-road air monitors in place of near-road monitors is supported by the facts that pollutants primarily emitted from sources other than traffic, such as PM_{10}, display a pattern very different from that for the other 3 pollutants (NO_2, $PM_{2.5}$ and O_3). On-road monitors successful detected PM_{10} concentrations near highway as well as in the roadside community that are comparable to the regional background concentrations. $PM_{2.5}$ and O_3 detected by on-road monitors are also comparable to those detected near highway and less travelled streets in the roadside community. NO_2 concentrations detected by the on-road monitors varied from the roadside monitors due to the complex interactions with ambient temperature, vehicle emissions, and atmospheric chemical reactions. Nevertheless, NO_2 concentrations observed near highway and in the community were far less than the NAAQS and are therefore less a concern in exposure studies.

REFERENCES

[1] J. Aguilera *et al.*, "Land-Use Regression of Long-Term Transportation Data on Metabolic Syndrome Risk Factors in Low-Income Communities," *Transp. Res. Rec.*, vol. 2675, no. 11, p. 40, Jul. 2021, doi: 10.1177/03611981211021853.

[2] L. V Giles and M. S. Koehle, "The health effects of exercising in air pollution.," *Sports Med.*, vol. 44, no. 2, pp. 223–249, Feb. 2014, doi: 10.1007/s40279-013-0108-z.

[3] K. W. Rundell and R. Caviston, "Ultrafine and fine particulate matter inhalation decreases exercise performance in healthy subjects.," *J. strength Cond. Res.*, vol. 22, no. 1, pp. 2–5, Jan. 2008, doi: 10.1519/JSC.0b013e31815ef98b.

[4] P. T. Cutrufello, J. M. Smoliga, and K. W. Rundell, "Small things make a big difference: particulate matter and exercise.," *Sports Med.*, vol. 42, no. 12, pp. 1041–1058, Dec. 2012, doi: 10.1007/BF03262311.

[5] N. A. H. Janssen, P. H. N. Van Vliet, H. Harssema, and B. Brunekreef, "Assessment of exposure to traffic related air pollution of children attending schools near motorways," vol. 35, no. 2, pp. 3875–3884, 2001.

[6] A. Spira-Cohen, L. C. Chen, M. Kendall, R. Lall, and G. D. Thurston, "Personal exposures to traffic-related air pollution and acute respiratory health among Bronx schoolchildren with asthma.," *Environ. Health Perspect.*, vol. 119, no. 4, pp. 559–565, Apr. 2011, doi: 10.1289/ehp.1002653.

[7] S. Kingsley *et al.*, "Proximity of US Schools to Major Roadways: a Nationwide Assessment," *J. Expo. Sci. Environ. Epidemiol.*, vol. 24, Feb. 2014, doi: 10.1038/jes.2014.5.

[8] A. Iannuzzi *et al.*, "Air pollution and carotid arterial stiffness in children.," *Cardiol. Young*, vol. 20, no. 2, pp. 186–190, Apr. 2010, doi: 10.1017/S1047951109992010.

[9] R. X. Armijos, M. M. Weigel, O. B. Myers, W.-W. Li, M. Racines, and M. Berwick, "Residential exposure to urban traffic is associated with increased carotid intima-media thickness in children.," *J. Environ. Public Health*, vol. 2015, p. 713540, 2015, doi: 10.1155/2015/713540.

[10] F. D. Gilliland *et al.*, "The effects of ambient air pollution on school absenteeism due to respiratory illnesses.," *Epidemiology*, vol. 12, no. 1, pp. 43–54, Jan. 2001, doi: 10.1097/00001648-200101000-00009.

[11] L. Chen, B. L. Jennison, W. Yang, and S. T. Omaye, "Elementary school absenteeism and air pollution.," *Inhal. Toxicol.*, vol. 12, no. 11, pp. 997–1016, Nov. 2000, doi: 10.1080/08958370050164626.

[12] J. K. Wendt, E. Symanski, T. H. Stock, W. Chan, and X. L. Du, "Association of short-term increases in ambient air pollution and timing of initial asthma diagnosis among Medicaid-enrolled children in a metropolitan area," *Environ. Res.*, vol. 131, pp. 50–58, May 2014, doi: 10.1016/j.envres.2014.02.013.

[13] F. Barone-Adesi *et al.*, "Long-Term Exposure to Primary Traffic Pollutants and Lung Function in Children: Cross-Sectional Study and Meta-Analysis," *PLoS One*, vol. 10, no. 11, pp. e0142565–e0142565, Nov. 2015, doi: 10.1371/journal.pone.0142565.

[14] U. Gehring *et al.*, "Traffic-related air pollution and respiratory health during the first 2 yrs of life.," *Eur. Respir. J.*, vol. 19, no. 4, pp. 690–698, Apr. 2002, doi: 10.1183/09031936.02.01182001.

[15] D. Ierodiakonou *et al.*, “Ambient air pollution, lung function, and airway responsiveness in asthmatic children.,” *J. Allergy Clin. Immunol.*, vol. 137, no. 2, pp. 390–399, Feb. 2016, doi: 10.1016/j.jaci.2015.05.028.
[16] J. Forns Guzman *et al.*, “Traffic-Related Air Pollution, Noise at School, and Behavioral Problems in Barcelona Schoolchildren: A Cross-Sectional Study,” *Environ. Health Perspect.*, vol. 124, Aug. 2015, doi: 10.1289/ehp.1409449.
[17] S. Lovinsky-Desir *et al.*, “Locations of Adolescent Physical Activity in an Urban Environment and Their Associations with Air Pollution and Lung Function.,” *Ann. Am. Thorac. Soc.*, vol. 18, no. 1, pp. 84–92, Jan. 2021, doi: 10.1513/AnnalsATS.201910-792OC.
[18] H. L. Brantley, G. S. W. Hagler, E. S. Kimbrough, R. W. Williams, S. Mukerjee, and L. M. Neas, “Mobile air monitoring data-processing strategies and effects on spatial air pollution trends,” *Atmos. Meas. Tech.*, vol. 7, no. 7, pp. 2169–2183, 2014, doi: 10.5194/amt-7-2169-2014.
[19] S. Hankey and J. D. Marshall, “On-bicycle exposure to particulate air pollution: Particle number, black carbon, PM2.5, and particle size,” *Atmos. Environ.*, vol. 122, pp. 65–73, 2015, doi: https://doi.org/10.1016/j.atmosenv.2015.09.025.
[20] C. H. Yu, Z. Fan, P. J. Lioy, A. Baptista, M. Greenberg, and R. J. Laumbach, “A novel mobile monitoring approach to characterize spatial and temporal variation in traffic-related air pollutants in an urban community,” *Atmos. Environ.*, vol. 141, pp. 161–173, 2016, doi: https://doi.org/10.1016/j.atmosenv.2016.06.044.
[21] L. Minet, R. Gehr, and M. Hatzopoulou, “Capturing the sensitivity of land-use regression models to short-term mobile monitoring campaigns using air pollution micro-sensors.,” *Environ. Pollut.*, vol. 230, pp. 280–290, Nov. 2017, doi: 10.1016/j.envpol.2017.06.071.
[22] G. R. McKercher and J. K. Vanos, “Low-cost mobile air pollution monitoring in urban environments: a pilot study in Lubbock, Texas.,” *Environ. Technol.*, vol. 39, no. 12, pp. 1505–1514, Jun. 2018, doi: 10.1080/09593330.2017.1332106.
[23] P. Wei *et al.*, “Determination of local traffic emission and non-local background source contribution to on-road air pollution using fixed-route mobile air sensor network,” *Environ. Pollut.*, vol. 290, p. 118055, 2021, doi: https://doi.org/10.1016/j.envpol.2021.118055.
[24] Y. Wu, Y. Wang, L. Wang, G. Song, J. Gao, and L. Yu, “Application of a taxi-based mobile atmospheric monitoring system in Cangzhou, China,” *Transp. Res. Part D Transp. Environ.*, vol. 86, p. 102449, 2020, doi: https://doi.org/10.1016/j.trd.2020.102449.
[25] T.-C. Lin, P.-T. Chiueh, S. M. Griffith, C.-C. Liao, and T.-C. Hsiao, “Deployment of a mobile platform to characterize spatial and temporal variation of on-road fine particles in an urban area,” *Environ. Res.*, vol. 204, p. 112349, 2022, doi: https://doi.org/10.1016/j.envres.2021.112349.
[26] R. Smit, P. Kingston, D. W. Neale, M. K. Brown, B. Verran, and T. Nolan, “Monitoring on-road air quality and measuring vehicle emissions with remote sensing in an urban area,” *Atmos. Environ.*, vol. 218, p. 116978, 2019, doi: https://doi.org/10.1016/j.atmosenv.2019.116978.
[27] Y. Chen *et al.*, “A new mobile monitoring approach to characterize community-scale air pollution patterns and identify local high pollution zones,” *Atmos. Environ.*, vol. 272, p. 118936, 2022, doi: https://doi.org/10.1016/j.atmosenv.2022.118936.
[28] B. Zhao *et al.*, “Urban Air Pollution Mapping Using Fleet Vehicles as Mobile Monitors

and Machine Learning," *Environ. Sci. Technol.*, vol. 55, no. 8, pp. 5579–5588, Apr. 2021, doi: 10.1021/acs.est.0c08034.
[29] R. W. Baldauf, V. Isakov, P. Deshmukh, A. Venkatram, B. Yang, and K. M. Zhang, "Influence of solid noise barriers on near-road and on-road air quality," *Atmos. Environ.*, vol. 129, pp. 265–276, 2016, doi: https://doi.org/10.1016/j.atmosenv.2016.01.025.
[30] Y. Shi, K. K.-L. Lau, and E. Ng, "Developing Street-Level PM2.5 and PM10 Land Use Regression Models in High-Density Hong Kong with Urban Morphological Factors," *Environ. Sci. Technol.*, vol. 50, no. 15, pp. 8178–8187, Aug. 2016, doi: 10.1021/acs.est.6b01807.
[31] A. A. Karner, D. S. Eisinger, and D. A. Niemeier, "Near-roadway air quality: Synthesizing the findings from real-world data," *Environ. Sci. Technol.*, vol. 44, no. 14, pp. 5334–5344, 2010, doi: 10.1021/es100008x.
[32] A. Venkatram, M. Snyder, V. Isakov, and S. Kimbrough, "Impact of wind direction on near-road pollutant concentrations," *Atmos. Environ.*, vol. 80, pp. 248–258, 2013, doi: 10.1016/j.atmosenv.2013.07.073.
[33] T. A. Cahill *et al.*, "Artificial ultra-fine aerosol tracers for highway transect studies," *Atmos. Environ.*, vol. 136, pp. 31–42, 2016, doi: 10.1016/j.atmosenv.2016.03.058.
[34] M. W. Tessum, L. Sheppard, T. V Larson, T. R. Gould, J. D. Kaufman, and S. Vedal, "Improving Air Pollution Predictions of Long-Term Exposure Using Short-Term Mobile and Stationary Monitoring in Two US Metropolitan Regions," *Environ. Sci. Technol.*, vol. 55, no. 6, pp. 3530–3538, Mar. 2021, doi: 10.1021/acs.est.0c04328.
[35] 2B Technologies, "NO2/NO/NOx Monitor Operation Manual," 2017.
[36] 2B Technologies, "Ozone Monitor Operation Manual," 2017.
[37] GRIMM, "Specification for portable laser aerosol spectrometer and dust monitor Model 1.108/1.109," *Users Man.*, p. 11, 2010.
[38] W. W. Li *et al.*, "Analysis of temporal and spatial dichotomous PM air samples in the El Paso-Cd. Juarez air quality basin," *J. Air Waste Manag. Assoc.*, vol. 51, no. 11, pp. 1551–1560, 2001, doi: 10.1080/10473289.2001.10464377.
[39] J. H. García *et al.*, "Characterization and implication of potential fugitive dust sources in the Paso del Norte region," *Sci. Total Environ.*, vol. 325, no. 1–3, pp. 95–112, 2004, doi: 10.1016/j.scitotenv.2003.11.011.